NeuroImage 279 (2023) 120335

Contents lists available at ScienceDirect

NeuroImage

journal homepage: www.elsevier.com/locate/ynimg

Review

Neural networks underlying visual illusions: An activation likelihood estimation meta-analysis

Alessandro von Gal [a,1,*], Maddalena Boccia [a,b], Raffaella Nori [c], Paola Verde [d], Anna Maria Giannini [a], Laura Piccardi [a,e,1]

[a] Department of Psychology, Sapienza University of Rome, Rome, Italy
[b] Cognitive and Motor Rehabilitation and Neuroimaging Unit, IRCCS Fondazione Santa Lucia, Rome, Italy
[c] Department of Psychology, University of Bologna, Bologna, Italy
[d] Italian Air Force Experimental Flight Center, Aerospace Medicine Department, Pratica di Mare, Rome, Italy
[e] San Raffaele Cassino Hospital, Cassino, FR, Italy

ARTICLE INFO

Keywords:
Visual illusions
Visual perception
Perceptual inference
ALE meta-analysis
fMRI
Schizophrenia
Lewy body dementia
Alzheimer's disease

ABSTRACT

Visual illusions have long been used to study visual perception and contextual integration. Neuroimaging studies employ illusions to identify the brain regions involved in visual perception and how they interact. We conducted an Activation Likelihood Estimation (ALE) meta-analysis and meta-analytic connectivity modeling on fMRI studies using static and motion illusions to reveal the neural signatures of illusory processing and to investigate the degree to which different areas are commonly recruited in perceptual inference. The resulting networks encompass ventral and dorsal regions, including the inferior and middle occipital cortices bilaterally in both types of illusions. The static and motion illusion networks selectively included the right posterior parietal cortex and the ventral premotor cortex respectively. Overall, these results describe a network of areas crucially involved in perceptual inference relying on feed-back and feed-forward interactions between areas of the ventral and dorsal visual pathways. The same network is proposed to be involved in hallucinogenic symptoms characteristic of schizophrenia and other disorders, with crucial implications in the use of illusions as biomarkers.

1. Introduction

The study of visual illusions dates back millennia; Aristotle himself is thought to be the first to have described the motion after-effect phenomena around 350 years B.C. (Eagleman, 2001; Wade, 2017). Despite being a matter of study for many centuries, the definition of visual illusions is still debated and continues to stimulate research and accounts across different disciplines. Generally speaking, illusions are usually considered as phenomena that generate a conflict between perception and our conception of reality (Shapiro and Todorovic, 2017). Definitions like these do not come without issues, because, in a sense, all vision is an illusion (Eagleman, 2001). Indeed, several accounts question the very notion of illusion, stating that the attempt to classify percepts as "veridical" or "illusory" may be misleading and inadequate (Purves et al., 2017; Rogers, 2022): since no experience copies reality (Boring, 1942) arguing about the correspondence to the "real" world plays no role in explaining perception. On the other hand, also the categorization of illusions comes with some issues. Several classification systems have been proposed across centuries, Vicario (2011) listed at least 26 classical ones, and more are still being proposed to this day (Coren et al., 1976; Gregory, 1997; Hamburger, 2016; Koenderink, 2017; Men'shikova, 2012; Westheimer, 2008). For example, Todorović (2020) proposed a new "augmented framework" based on 4 families of phenomenological criteria, with specific interest on the importance of contextual information. Recently, Rogers (2022) criticized this framework, arguing that visual illusions should be thought as stimuli that give rise to perceptual effects that are coherent and reflect just how the perceptual system works, implying that we call "illusions" the ones that give rise to a percept for which we have yet to find a satisfactory explanation. Conversely, Hamburger (2016) argues that there is a need to go beyond the previous classification systems mainly based on phenomena, and to classify different types of visual illusions based on the underlying cognitive mechanisms and neural cause that gives rise to them, possibly in accordance with Rogers' account.

* Corresponding author.
E-mail address: alessandro.vongal@uniroma1.it (A. von Gal).
[1] https://spatialcognitionlab.com

https://doi.org/10.1016/j.neuroimage.2023.120335
Received 13 April 2023; Received in revised form 5 July 2023; Accepted 14 August 2023
Available online 15 August 2023

Besides the epistemological debate on the nature and phenomenological classification of illusions, illusory visual configurations have long been used as research tools in psychology research since they have the potential to open a window into the neurobiology of visual perception (Eagleman, 2001; Hamburger, 2016; Spillmann, 2009) and to reveal the top-down probabilistic inferential processes involved during perceptual processing (Clark, 2013; Friston, 2005a; O'Reilly et al., 2012).

1.1. Visual illusions along the ventral and dorsal pathways

Ungerleider and Mishkin were the first to propose the anatomical distinction between a "what" ventral and "where" dorsal anatomical pathways in the macaque brain (Mishkin et al., 1983; Ungerleider, 1982). The first being responsible for representing objects, thus underlying "object vision"; the second, involved in representing the spatial location of objects, thus involved in "spatial vision". Following this conceptualization, Goodale and Milner went on to propose a similar functional division of labor in the human brain (Goodale and Milner, 1992; Milner and Goodale, 1995, 2006). The resulting perception-action model has its roots in the evidence coming from the double dissociation between visual form agnosia, resulting from lesions along the ventral pathway and characterized by impairments in building object representations but with spared ability in grasping them (Goodale et al., 1994); and optic ataxia, characterized by difficulties in acting upon object despite an intact ability to represent them correctly following dorsal lesions (Goodale et al., 1994). Thus, the "What & How" functional model describes an occipito-temporal ventral pathway, projecting from V1 to the inferotemporal cortex mediating conscious perception, object recognition and scene parsing, and an occipito-parietal dorsal pathway, projecting from V1 to the posterior parietal cortex and subtending the visual control of actions, or "vision-for-action".

In the attempt to characterize the properties belonging to the two pathways, a considerable number of studies observed the differential processing of the pathways in response to visual illusory configurations. In its early conceptualization, the model implied that object perception and memory-guided movements are highly sensitive to contextual illusions while visually guided movements remain unaffected by these, leading to the proposal that the dorsal visual stream is "immune" to contextual illusory effects (Milner and Goodale, 2008).

Pivotal evidence for this model came from Aglioti et al. (1995), who showed that participants experienced the contextual effects induced by the Ebbinghaus-Titchener illusion when they had to estimate the size of the target. Noteworthy, when they were asked to grasp the target, their motor estimation of the size of the circle target (measured as grip size) was unaffected by contextual illusory inducers and remained metrically accurate, correctly matching the dimensions of the target. However, later evidence did not confirm this result when the perceptual and motor tasks were operated on a single Ebbinghaus figure (Pavani et al., 1999) and when visual feedback was controlled (Bruno and Franz, 2009; Franz et al., 2000). Moreover, motor aspects involved in grasping seem to be based on object properties coded ventrally and affected by size (Gallivan et al., 2014), thus suggesting an interaction between the two functional pathways. In the same vein, Chen and colleagues (2022) found that the manipulability of a target object at the center of the Ebbinghaus figure modulates the magnitude of the illusion, and that this effect is associated with reciprocal effective connectivity between the LOC and SPL in the left hemisphere. Further evidence came from studies on visuomotor updating. Medendorp and colleagues (2018) recorded saccades during the presentation of Müller-Lyer and Brentano illusions. Particularly, by using a double-step saccade task they were able to test whether visuomotor updating was affected by the illusion and found that the second saccade was actually based on an updated but illusory target. Thus, the evidence that visuomotor updating, which depends on the activity of the dorsal pathway, is affected by the contextual illusion was further confirmed by a selective modulation in the BOLD signal in areas V7, intraparietal sulcus and frontal eye fields related to the effect of the illusion. Following this evidence, they argue that the dorsal pathway represents perceived target locations instead of physical target locations, since areas along the dorsal pathway are directly sensitive to contextual illusions independently from an interaction with the ventral pathway, leading them to the conclusion that functional specializations of the dorsal and ventral visual stream are relative rather than absolute. Neuropsychological reports also support the relative functional specialization of the two streams. Coello et al. (2007) reported the case of a patient with a bilateral lesion of the dorsal pathway in most of POJ and mIPS, resulting in difficulties mainly involving grasping and reaching movements, typical of Optic Ataxia, which disappeared under visual control. Surprisingly, the patient did not show any differences compared to healthy participants in both perceptual judgements and motor actions when acting on a Roelofs illusion configuration and on a Titchener-Ebbinghaus illusion. In fact, neither the control participants' nor the patient's grip aperture was affected by the Ebbinghaus illusory contextual configuration, seemingly confirming the early results of Aglioti and colleagues (1995). Regardless, the absence of perceptual and motor differences between the patient with the lesion of the dorsal stream and the healthy controls lead them to conclude that a distinction of visual processing for perception and action is unlikely to depend on a simple segregation between dorsal and ventral visual pathways.

Conversely, de la Malla and colleagues (2019) described a patient with a bilateral occipito-temporal lesion with a completely spared dorsal pathway resulting in visual form agnosia, characterized by issues in representing objects' features (for a detailed description see Heywood et al., 1991). He was asked to attend to a gabor patch embedded with motion, thus inducing a motion illusion affecting the target's apparent position, direction and speed (de la Malla et al., 2018). They demonstrate that the patient is able to report object motion, thus concluding that motion related perceptual judgements do not depend on the functioning of the ventral pathway. Moreover, they show that the motion illusion affects both perception judgements and action equally in the patient and controls; thus, demonstrating that the dorsal pathway actually is affected by illusions and is responsible for both perceptual and motor processing related to movement. Based on this evidence, they conclude that it is the visual attribute that determines where the information will be processed, not whether the information is used for perception or action. Overall, these evidence point towards interconnected dynamic networks, with ventral and dorsal streams sharing various processing characteristics (e.g. de Haan and Cowey 2011, Galletti and Fattori 2018, Pavani et al. 1999, Sulpizio et al. 2020).

In the present study we performed an Activation Likelihood Estimation (ALE) meta-analysis on previous functional imaging studies that employed illusory configurations; with a two-fold aim:

i) to describe the overarching neural networks of commonly activated areas underlying the processing of illusory contours, geometrical and motion illusions.
ii) to contribute to the debate about the classical distinction between ventral and dorsal visual processing by comparing the network of commonly activated areas in response to static illusory configurations and motion-related visual illusions.

The first subgroup of studies included experiments investigating the neural bases of optical illusions such as Müller-Lyer, Ebbinghaus, Illusory Contours, Ponzo and Roelofs illusion and others. These visual configurations mainly elicit the illusory perception of features (e.g., shape and length) expected to be processed in the ventral pathway according to the perception-action model. On the other hand, we pooled a second sub-group of studies that included only the experiments investigating the neural bases of motion-related visual illusions. Differently, the illusory percepts resulting from these visual configurations involve features (e.g., depth, motion, position change) expected to be processed along the dorsal visual pathway. Hence, the comparison between the two networks of overlapping activations can be used to test the

predictions of the classic perception-action model and disentangle the question on whether or not the two types of processing involve completely separated functional routes or if visual perception depends on dynamic interactions between the two streams. Following this rationale, if the strict feed-forward accounts are correct then we expect to find a clear distinction between ventral and dorsal visual areas, selectively associated with static and motion illusions, respectively. Conversely, if the interaction accounts are correct, then the results are expected to show regions distributed along both the pathways independently of the type of illusory processing, with shared areas between the two networks.

2. Materials and methods

2.1. Inclusion criteria for papers

We employed a systematic approach to identify the papers that best suited the aim of the current meta-analysis following the Preferred Reporting Items for Systematic Reviews and Meta-Analyses (PRISMA) guidelines (Page et al., 2021). The search of relevant papers was conducted on PubMed, Scopus and Web of Knowledge (Web of Science) between July and August 2022. The following query was searched in all of the three databases: (((visual OR optical) AND illusion*) OR illusory) AND (fMRI OR "functional magnetic resonance imaging"), resulting in a total of 1,445 results. Duplicates were then removed, leaving 771 records.

Of these remaining records, only the ones that met the following a priori inclusion criteria were kept: (1) only studies employing whole-brain analyses using functional magnetic resonance imaging (fMRI); (2) studies had to provide activation foci either in the Montreal Neurological Institute (MNI) or Talairach reference frames; (3) studies had to be conducted only on young and healthy participants, (4) without any pharmacological manipulation; (5) experiments had to present participants with context dependent visual illusions, meant as visual configurations that induced a consistent and univocal illusory percept among subjects; thus studies using multisensory and bistable illusions, or adaptation and after effects, were excluded; (6) visual illusions proposed to participants had to be perceivable from a single perspective and did not require the participant to move in order to appreciate them.

The record screening was conducted by one investigator (AvG), and records were successively rechecked by a second independent investigator. The selection process resulted in 23 eligible papers, 4 of which had to be excluded since they did not report the coordinates of the foci of activation. Finally, those included in the meta-analysis were extracted from the remaining 19 papers; 11 of these were related to static illusions, while the other 8 were on motion illusions; leading to a total of 41 experiments analyzed in the General ALE, 28 in the Static ALE and 13 in the Motion ALE. The flow-chart describing the screening process of eligible papers is shown in Fig. 1, while Table 1 summarizes the studies from which the contrasts were extracted.

2.2. Activation likelihood estimation

To understand how the processes involved in building different types of illusory percepts are distributed among cortical areas, we employed an Activation Likelihood Estimation analysis (ALE) (Laird et al., 2009;

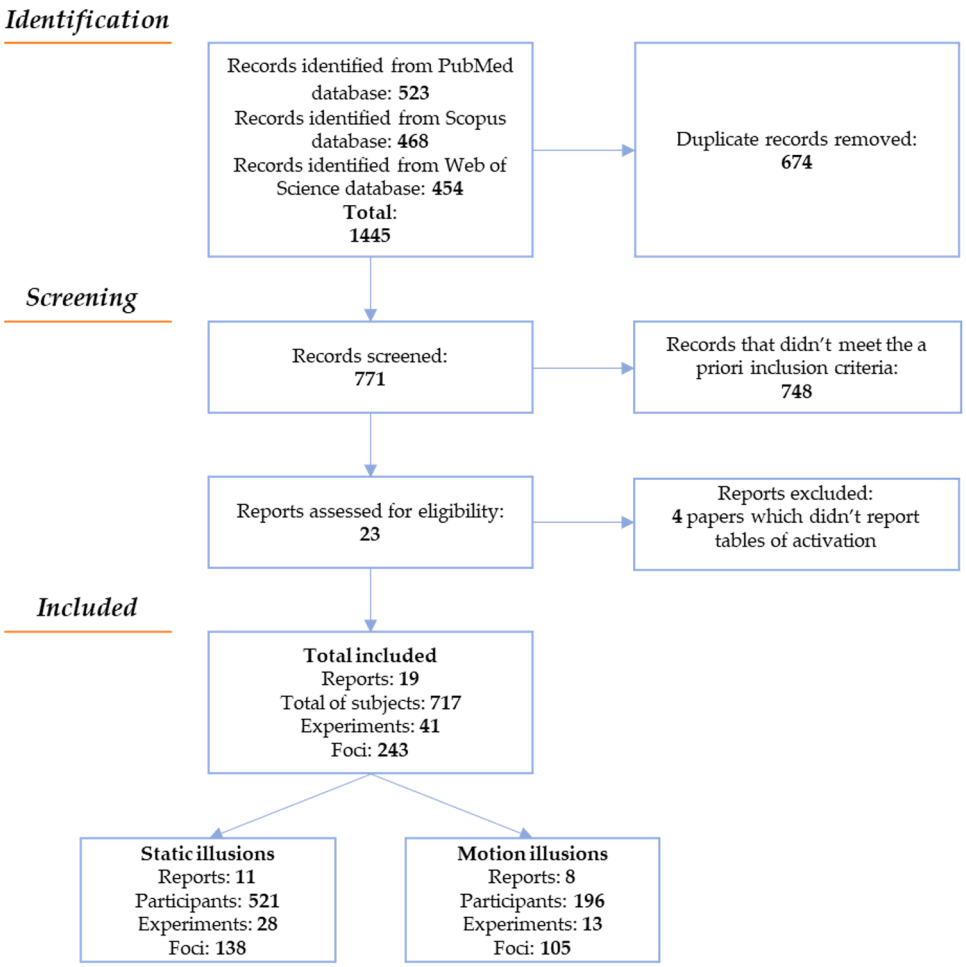

Fig. 1. Flowchart showing the steps of the paper selection process. Detailed information about the inclusion criteria is described in paragraph 2.1.

Table 1
Complete list of papers considered for the meta-analysis. Details about the number of subjects (N), the number of contrasts, the number of resulting foci of activation, the type of illusion used in the study and the contrasts selected for the meta-analyses.

Papers	N	Experiments	Foci	Illusion	Contrasts
Static					
Chen et al., 2021	20	2	11	Illusory contours	Kanizsa figure > Baseline (rotated inducers); Interaction: Configuration (Kanizsa > Basline) x Task (Luminance discrimination vs Spatial localization)
Chen et al., 2022	30	4	33	Ebbinghaus illusion	Ebbinghaus (non-manipulable central target with large inducers) > control (inducers and target presented asynchronously); Ebbinghaus (non-manipulable central target with small inducers) > control (inducers and target presented asynchronously); Ebbinghaus (manipulable central target with large inducers) > control (inducers and target presented asynchronously); Ebbinghaus (manipulable central target with small inducers) > control (inducers and target presented asynchronously)
Kreutzer et al., 2015	23	2	6	Ebbinghaus illusion	Conjunction: Ebbinghaus absent > present AND small adaptor > large adaptor; Interaction: [(adaptor present/Ebbinghaus absent − adaptor absent/Ebbinghaus absent) − (adaptor present/Ebbinghaus present −adaptor absent/Ebbinghaus present)]
Murray et al., 2002	5	1	4	Illusory contours	Illusory contours > control (rotated inducers)
Plewan et al., 2012	21	3	9	Müller-Lyer (Brentano) illusion	Illusion strength (parametric contrast); Differential effect of illusion strength (Landmark task > Luminance task); Landmark task > Luminance task
Ritzl et al., 2003	11	2	4	Illusory contours	Illusory contours > Explicit contours; Illusory contours > Inferred contours (rotated inducers)
Shen et al., 2016	15	6	22	Poggendorf, Illusory contours	Poggendorf (real contours) > control (no poggendorf); Illusory contours > control (rotated inducers); Interaction: Poggendorf x Illusory contours; Poggendorf (parametic contrast); Illusory contours (parametric contrast); Differential effect related to Poggendorf (Parametric Poggedorf > Parametric Illusory contours)
Tabei et al., 2015	18	3	36	Müller-Lyer, Ponzo, Hefler, Zerbino, Ebbinghaus, Jastrow, Delboeuf	Shape task (identified) > Baseline; Shape task (not identified) > Baseline; Shape task > Word task
Walter and Dassonville, 2008	16	1	3	Roelofs effect	Conjunction: [(location with frame) > (location without frame)] and [(location with frame) > (color with frame)]
Weidner and Fink, 2007	15	3	6	Müller-Lyer (Brentano)	Landmark task > Luminance task; Illusion strength (parametric contrast); Interaction: Illusion strength x Task
Weidner et al., 2014	20	1	4	Moon illusion	Interaction: [(Moon low with scene – Moon high with scene) – (Moon low without scene–Moon high without scene)]
Motion					
Budnik et al., 2016	16	1	1	Pinna figure	Illusory rotation > Non-rotating figure
Fraedrich et al., 2010	18	1	6	Self-motion illusion	Self-motion illusion > control (scrambled)
Hamm et al., 2014	18	3	25	Illusory line motion	Illusory line motion > real motion; Illusory line motion (parametric contrast); Reverse illusory line motion (parametric contrast)
Kovacs et al., 2008	10	1	5	Self-motion illusion	Illusory self motion > Object motion (random moving dots)
Riedel et al., 2005	11	1	8	Autokinetic illusion	Autokinetic illusion > Static condition
Tanaka and Yotsumoto, 2016	16	1	8	Wriggling motion trajectory illusion	Illusory shift direction > Moving dots (non-inducing)
van der Hoorn et al., 2010	15	3	22	Self-motion illusion	Forward optic flow > Stationary control; Reverse optic flow > Stationary control; Forward optic flow > Reverse optic flow
Yamamoto et al., 2008	13	2	30	Stereokinetic depth illusion	Peripheral stereokinetic illusion > control (non-illusion inducing moving circles); Central stereokinetic illusion > control (non-illusion inducing moving circles)
Total	311	41	243		

Turkeltaub et al., 2002). This approach is a coordinate-based meta--analysis and, as such, consists in taking the activation foci extracted from the records of interest and creating a probability distribution around the reported peak. The algorithm then generates ALE maps by testing the null hypothesis that activation foci are uniformly spread across the whole brain, under the assumption that each voxel has the same probability of being activated. Thus, ALE maps are obtained by computing the union of activation probabilities for each voxel, returning a map of significant spatial convergence among the contrasts of interest.

Contrast of interest were selected from the eligible papers, only the foci reflecting the activity related to the processing of illusory percepts were selected. These were double-checked by an independent observer to avoid selection bias and risk of excluding potentially valid contrasts. We first performed a general ALE meta-analysis including all foci from the two types of illusions for a total of 243 foci reported in 41 experiments. Afterwards, two separate meta-analyses were conducted in which contrasts were divided depending on the type of the illusion employed in the task. These were referred to as: “static” if the percept involved processing of static spatial features (object-related features such as shape, length etc.); “motion” if the illusory percept involved illusory motion or motion-related illusory changes (e.g., depth, direction etc.). Fig. 2 shows the static and motion illusions employed in the studies considered in the present analysis.

After computing separate ALE meta-analyses related to the two types of illusions, we computed a contrast analysis between the two to spatial convergence related to the stimuli categories. Moreover, we also computed a conjunction analysis to find the common areas subtending to the processing of both types of illusion.

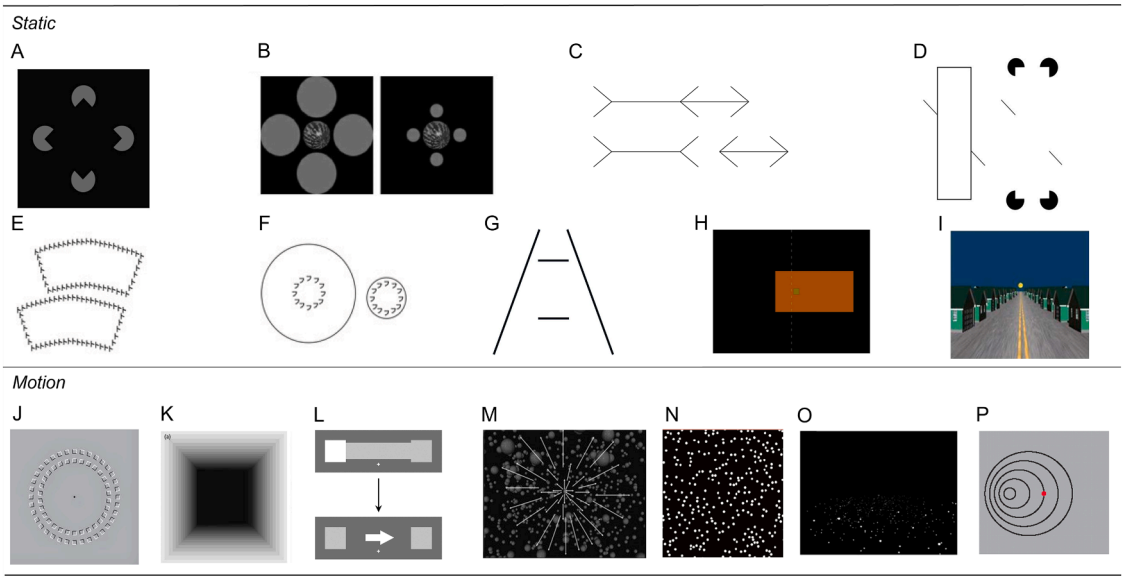

Fig. 2. Image showing the types of illusions employed in the studies included in the current meta-analysis. The upper part shows the following static illusions: **A**. Illusory contours. The grey pac-man-like inducers generate the illusory percept of a diamond shape (taken from Chen et al. 2021). **B**. Ebbinghaus illusion. Even though the size of the central circle is the same in the two panels, the one on the right seems larger because of the smaller circles surrounding it (variant with real object as central target used in Chen et al. 2022). **C**. Brentano variant (upper) and Muller-Lyer illusion (lower). The length of the segment between the angles on the left seems longer than the portion between the angles on the right, even though they have the same length. **D**. Poggendorf illusion. Two collinear segments separated by a parallel seem to be non-collinear even though they are. The right side shows the same illusion combined with illusory contours (as used in Shen et al. 2016). **E**. Jastrow illusion. The lower shape seems to be longer than the upper one, even though they are the same size. Variant in which the shapes are made of kanji letters (as used in Tabei et al. 2015). **F**. Delboeuf illusion. The internal circle on the right seems larger that the internal circle on the left, but they are the same. As in the previous illusion, the circles are made of kanji letters (Tabei et al. 2015). **G**. Ponzo illusion. The two lines have the same length but the lower seems to be longer than the upper one. **H**. Roelofs effect. The green square enclosed in the orange frame seems to be located further on the left relative to the midsagittal plane (i.e., the dotted line, not shown to participants) (Walter and Dassonville, 2008). **I**. Moon Illusion. The moon (yellow circle) seems to be larger when it is closer to the horizon (taken from Weidner et al. 2014). The last row shows the motion-related illusions: **J**. Stereokinetic effect. The two circles seem to move in opposite directions when the configuration moves towards or away from the viewer. **K**. Self-motion illusion. Frame of a video inducing illusory self forward motion and changes in direction inside a tunnel (taken from Fraedrich et al. 2010). **L**. Illusory line motion. When a luminance flash precedes the sudden disappearance of a bar, the bar seems to be drawn in motion away from the location of the flash (Hamm et al. 2014). **M**. Self-motion illusion. Coherent optic flow induces the illusion of moving of the self. Arrows show the direction in which the dots move in the video (taken from Kovacs et al. 2008). **N**. Wriggling Motion Illusion. Dots moving randomly in straight lines seem to curve if they never overlap with each other; when allowed to overlap the illusory shift in direction disappears (taken from Tanaka and Yotsumoto 2016). **O**. Self-motion illusion. Illusory self-motion elicited by dots moving towards the observer in the lower visual field (taken from van der Hoorn et al. 2010). **P**. Stereokinetic depth illusion. Two-dimensional moving circles induce the illusion of depth (taken from Yamamoto et al. 2008).

We used the GingerALE 3.0.2 software (http://brainmap.org/ale/) to conduct these analyses. First, all coordinates were automatically converted to MNI using GingerALE Talaraich to MNI (SPM) built in converter. Then, the software computes the FHWM describing the uncertainty of spatial location (i.e., the probability distribution) of each focus, for each experiment. Afterwards, model activation (MA) maps are computed for each voxel by taking the voxel-wise union of the modeled probability values of all foci, for each experiment. These MA maps represent the summary of the results reported in a specific study considering the spatial uncertainty associated with the reported foci coordinates. ALE scores are then computed as the union of these probabilities across experiments for each. These scores are tested against the null distribution calculated for each voxel, reflecting a random spatial association of the MA across experiments (Eickhoff et al., 2009, 2012). The resulting thresholded ALE map was then computed using a cluster forming threshold of $p < 0.001$ and a cluster-level threshold of $p < 0.05$ Family Wise Error (FWE) corrected (Eickhoff et al., 2016). AAL3 (Rolls et al., 2020) and HCP (Glasser et al., 2016) functional atlases had been used to describe the results of the present meta-analyses.

2.2. Meta analytic connectivity modeling (MACM)

To support the findings emerging from the previous analyses we performed meta-analytic connectivity modeling (MACM) using the regions resulting from the conjunction analysis as seeds. This allowed us to identify the regions that are significantly co-activated with the seed region at a level above chance, extracted across a consistent number of neuroimaging studies (Eickhoff et al., 2011; Robinson et al., 2009). To do this, we searched all the articles that included at least one voxel of the seed region in the BrainMap database using Sleuth (http://www.brainmap.org/sleuth/) and we conducted another ALE meta-analysis on all the foci reported in the experiments resulting from the search. The MACM analysis' results represent the areas of significant co-activation of other voxels with one seed region, thus, depicting a measure of functional interactions between one region and other cortical modules based on their whole-brain co-activations patterns (Eickhoff et al., 2011; Laird et al., 2013). As in the previous analyses, the ALE map was thresholded at $p < 0.001$, cFWE corrected at $p < 0.05$.

3. Results

3.1. General ALE

The general ALE meta-analysis, which included all studies, identified a network of posterior and parietal areas distributed bilaterally (see Fig. 3, Table 2). The analysis revealed several peaks of overlapping activation, with the largest cluster observed in the right hemisphere. The first peak was found in the middle occipital gyrus (MOG) centered in correspondence of the lateral occipital area (LO1) and spreading in the third lateral occipital area (LO3), with activation extending ventro-

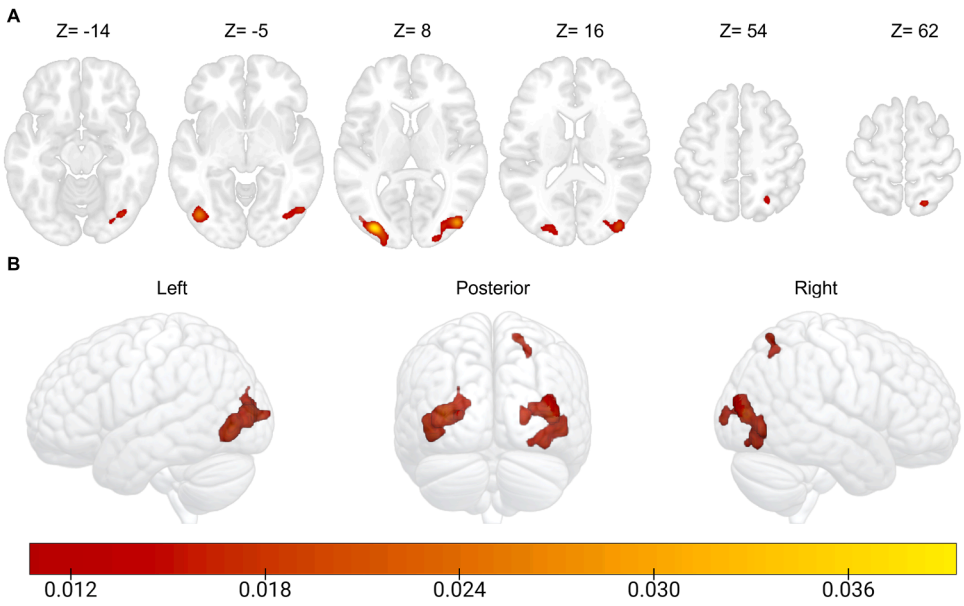

Fig. 3. Network of common activations resulting from the ALE meta-analysis. **A.** The different clusters of overlapping activation are presented overlayed on the MNI152 volume template. MNI coordinates (Z) are provided for each slice. **B.** The same results are shown on a 3D rendered brain from different views: left hemisphere view, posterior view of both hemispheres and right hemisphere view. The color bar represents the increasing degree of convergence expressed by the ALE values.

Table 2
Results of the general meta-analysis. For each cluster, the general brain region according to the AAL3 atlas and specific surface area according to the HCP parcellation, are provided where possible. Hemisphere, size of the cluster (in mm3), the ALE and its corresponding standardized Z value are also provided. MNI coordinates are reported for each peak present in the cluster.

Cluster	Region	Area	Hemisphere	Volume (mm^3)	ALE	Z	Coordinates		
							x	y	z
1	MOG	LO1	RH	8304	0.0293	6.041	44	-82	8
		V4			0.0207	4.8095	30	-86	10
	ITG	V4t			0.0177	4.324	50	-70	-4
	FFG	PIT			0.0176	4.3097	38	-74	-14
	MOG	V2			0.0173	4.2684	24	-98	4
	FFG	V4			0.014	3.7019	28	-82	-14
2	MOG	V3CD	LH	8016	0.0393	7.315	-34	-88	8
	IOG	LO2			0.0269	5.7038	-44	-76	-4
	MOG	V4			0.0158	4.0259	-22	-88	16
	SOG	*			0.0124	3.3977	-24	-88	26
3	SPG	VIP	RH	1056	0.0175	4.2988	20	-64	62
		MIP			0.0153	3.9274	26	-62	54

Notes. LH= Left Hemisphere; RH= Right Hemisphere. **Region labels**. MOG= Middle Occipital Gyrus; ITG = Inferior Temporal Gyrus; FFG= Fusiform Gyrus; IOG= Inferior Occipital Gyrus; SOG= Superior Occipital Gyrus; SPG= Superior Parietal Gyrus. **Area labels**. LO1= Lateral Occipital 1; V4= Fourth Visual Area; PIT= Posterior Infero Temporal cortex; V2= Secondary Visual Cortex; LO2= Lateral Occipital 2; VIP= Ventral IntraParietal Complex; MIP= Medial IntraParietal Area. The symbol "*" indicates that there was no area corresponding to the coordinates according to the HCP surface parcellation, indicating the possibility that the area was located underneath the surface.

laterally towards the inferior occipital (IOG), middle (MTG) and inferior temporal gyri (ITG) along the second lateral occipital area (LO2) and V4t. The cluster extended ventrally to include portions of PH and fusiform face complex (FFC), reaching two other peaks in the fusiform gyrus (FFG) on the ventral surface of the cortex, namely the posterior inferotemporal cortex (PIT) and V4, with a portion of V8 included in the cluster. A second part of the cluster extended medially inside the cortex and re-emerged in the MOG, descending from a small portion of PGp in the inferior parietal lobule (IPL) towards V4, comprehending parts of V3CD and V3, until reaching another peak centered in V2 and ending in V1. In the left hemisphere, converging activation was observed in the superior occipital gyrus (SOG) and included portions of V7 and V3A, with activation extending ventrally to reach another peak in V4 and continuing along the MOG. The cluster moved posteriorly from area V3CD to areas V4, V3 and V2, and extended ventro-laterally from the MOG, along areas V4, V4t, LO1 and LO2, to the IOG. Here, the included the inferior portion of LO2, areas PIT, PH, and a small portion of FFC in its inferior extreme. The last cluster was found in the right Superior Parietal Gyrus (SPG), with converging activation distributed around a first peak corresponding to the ventral intraparietal area (VIP) and included portions of areas 7Am and 7PL more medially. The cluster also included a second peak, namely the medial intraparietal area (MIP), and comprehended the superior part of the ventral lateral intraparietal area (LIPv) laterally.

3.2. *Static visual illusions*

The static ALE meta-analysis included only the contrasts representing the foci of activation related to the processing of optical illusions inducing a static percept. The analysis revealed a bilateral cluster of activation in the MOG, including functionally defined areas V4 and V3CD, and extending to neighboring areas V3 and LO1 ventrally. In the left hemisphere, the cluster also extended to a small portion of area V2 ventrally, as well as a portion of V3B and V3A superiorly, in the SOG. In the right hemisphere the cluster included a small portion of PGp. We also found activation in the right SPG, which extended to the superior portion of the IPG. This cluster extended medially from VIP including area 7Am and spread ventro-laterally to include the superior portion of the ventral Lateral IntraParietal area (LIPv) until reaching the second peak centered in MIP. Overlapping activation was also detected in the

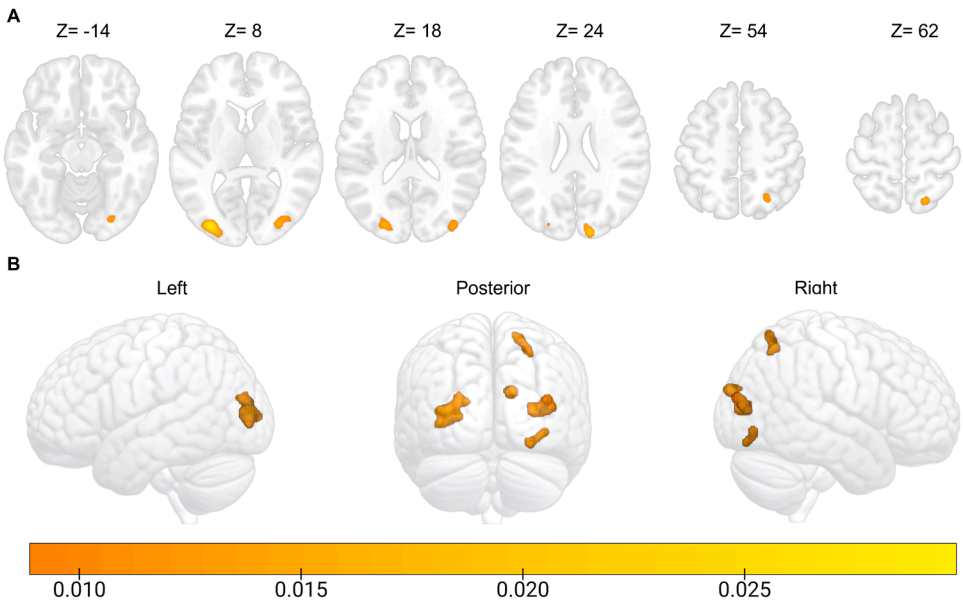

Fig. 4. Network of common activations resulting from the Static ALE meta-analysis. **A**. The different clusters of overlapping activation are presented overlayed on the MNI152 volume template. MNI coordinates (Z) are provided for each slice. **B**. The same results are shown on a 3D rendered brain from different views: left hemisphere view, posterior view of both hemispheres and right hemisphere view. The color bar represents the increasing degree of convergence expressed by the ALE values.

depths of the right IOG and possibly subcortically (see Fig. 4). Indeed, the HCP parcellation failed to identify a surface region corresponding to this peak. However, the cluster extended downwards, reaching two other peaks in area V4, on the ventral surface of the Fusiform Gyrus (FFG) and in the Lingual Gyrus (LING), extending to the neighboring area V8 and just a small portion of V3 (Fig. 4, Table 3).

3.3. Motion illusions

The motion ALE meta-analysis focused on contrasts that involved processing of motion-related optical illusions and identified clusters of overlapping activation in both hemispheres. In the left hemisphere, convergent activation extended downwards from the MOG to the IOG, with activation spreading along V4 and LO2. Around its upper boundaries, the cluster included small portions of adjacent areas such as MT, LO1 and LO2; while it included portions of the PIT, PH and FFC in its lower part. The same cluster extended anteriorly underneath the cortical surface, reaching a second peak in the MTG, where activation included most of area FST and a small portion of the ventralmost part of the second temporoparietal occipital junction (TPOJ2). In the right hemisphere, the first cluster showed overlapping activation in the MOG around the lower part of LO1, towards small portions of nearby areas MT and LO3, as well as LO2 area in its lower part. The cluster then extended ventro-laterally along V4t in the MTG, including portions of FST and PH, reaching the FFG, including the PIT and small portions of FFC and V8. Another cluster was detected across the right Precentral gyrus (PreCG) and the right opercular part of the Inferior frontal gyrus (IFGoperc). This showed a single main peak in the upper part of Rostral area 6 (6r), with activation extending towards the inferior part of the Premotor Eye Fields (PEF) and a lateral portion of area IFJp. The last cluster included portions of the SOG, MOG as well as the cuneus (CUN) where activation spread around a single peak in V2 and included a portion of the posterior part of V3 (Fig. 5, Table 3).

3.4. Conjunction analysis

The conjunction between the sub-meta-analyses [Static $\wedge$ Motion] revealed only two small bilateral activations in the left and right MOG; the second resulted to be particularly reduced in volume, compared to the first with peaks in the right V3CD and the left LO1 (Fig. 6, Table 4).

3.5. Contrast: motion > static

Finally, we calculated the contrast between the two meta-analyses to investigate the convergence of activation related to the processing of motion-related and static illusions. While the [Static > Motion] contrast did not reveal any significant overlapping activation; the [Motion > Static] contrast resulted in several clusters showing significantly higher convergence of activations in experiments that used motion-related illusions. In the left hemisphere, activation extended across the MOG in which most of the convergent activation was found along the whole V4t area, moving dorsally to MT and LO3, and ventrally to LO2. The cluster extended laterally underneath the surface reaching the MTG, re-emerging towards the surface in a small patch of overlapping activation found in the TPOJ2. Similarly, activation in the right hemisphere was detected in MT and stretched to LO3, LO1, and LO2 in the right MOG. From here, the area of overlapping activation extended ventro-laterally along V4t, crossing the right IOG until reaching FST in the ITG. Ventral to this cluster, another one extended across the right ITG and IOG, moving posteriorly from FST to PH and ending in FFC. Another cluster was found in the right frontal lobe, in the depths of the PreCG, including areas IFJp, 6r and PEF (Fig. 7, Table 5).

3.6. MACM functional connectivity

We conducted a MACM to further explore the functional interactions between the modules that emerged from the previous analyses. Specifically, the conjunction analysis confirmed consistent co-activation in the right LOC common to the sub-meta-analyses and coherent with the right lateralization of all the networks resulting from the previous analyses. Therefore, we built a spherical ROI with a 12mm radius centered in the peak coordinates of the cluster of activation found in the right MOG (see Table 4) using the Mango software (https://mangoviewer.com/). In the BrainMap database, we searched for all the fMRI experiments conducted on neurotypical subjects (i.e., Normal Mapping only, without any task constraint) that presented significant activation in at least one voxel included in our selected region. Therefore, we conducted a meta-analysis on 5524 foci extracted from 268 experiments, including a total of 3827 subjects (detailed information on the included contrasts can be found on the OSF repository, together with all the other data and analyses: https://osf.io/p5d9f/). The analysis revealed significant co-activations ($p < 0.05$ cFWE corrected) between our region and other cortical areas distributed bilaterally across hemispheres (Fig. 8,

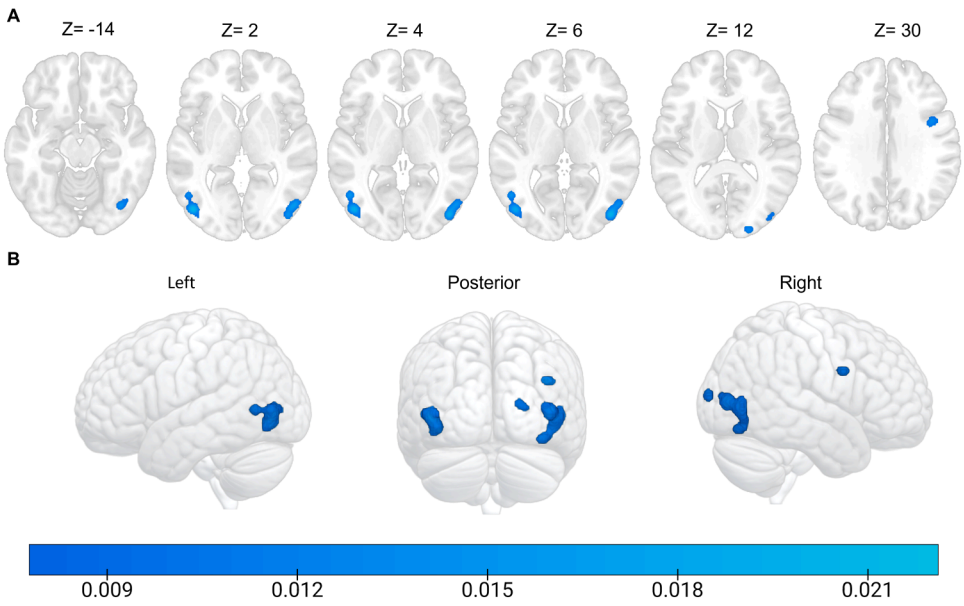

Fig. 5. Network of common activations resulting from the Motion ALE meta-analysis. **A.** The different clusters of overlapping activation are presented overlayed on the MNI152 volume template. MNI coordinates (Z) are provided for each slice. **B.** The same results are shown on a 3D rendered brain from different views: left hemisphere view, posterior view of both hemispheres and right hemisphere view. The color bar represents the increasing degree of convergence expressed by the ALE values.

Table 3
Results of the static and motion illusions meta-analyses. For each cluster, the general brain region according to the AAL3 atlas and specific surface area according to the HCP parcellation are provided where possible. Hemisphere, cluster size (in mm3), ALE value and its corresponding standardized Z value are also provided. MNI coordinates are reported for each peak present in the cluster.

Cluster	Region	Area	Hemisphere	Volume (mm^3)	ALE	Z	Coordinates		
							x	y	z
Static									
1	MOG	V3CD	LH	4256	0.0298	6.5204	-34	-88	8
		V4			0.0156	4.342	-24	-86	18
2	MOG	V4	RH	2824	0.0203	5.1111	30	-84	12
		V3CD			0.0151	4.245	42	-84	14
		*			0.015	4.216	40	-88	18
3	SPG	VIP	RH	1352	0.0172	4.623	20	-64	62
		MIP			0.0147	4.1563	26	-62	54
4	IOG	*	RH	1184	0.0143	4.0775	36	-78	-6
	FFG	V4			0.0139	4.0044	28	-82	-14
	LING	V4			0.0099	3.2837	22	-76	-8
5	CUN	V3	RH	928	0.0215	5.2998	14	-94	24
Motion									
1	MOG	LO1	RH	4424	0.0221	5.8686	44	-82	6
	MTG	V4t			0.0164	4.8527	50	-74	2
	FFG	PIT			0.0154	4.6803	38	-74	-14
2	MOG	V4t	LH	3456	0.0219	5.8339	-46	-78	2
	MTG	FST			0.0164	4.8626	-50	-64	4
3	PreCG	6r	RH	688	0.0137	4.3415	42	6	30
4	CUN /SOG	V2	RH	648	0.0134	4.2622	22	-96	12

Notes. LH= Left Hemisphere; RH= Right Hemisphere. **Region labels**. MOG= Middle Occipital Gyrus; SPG= Superior Parietal Gyrus; IOG= Inferior Occipital Gyrus; FFG= Fusiform Gyrus; LING= Lingual Gyrus; MTG= Middle Temporal Gyrus; PreCG= Precentral Gyrus; CUN= Cuneus. Area labels; SOG= Superior Occipital Gyrus. **Area labels**. V4= Fourth Visual Area; VIP= Ventral IntraParietal Complex; MIP= Medial IntraParietal Area; V3= Third Visual Area; LO1= Lateral Occipital 1; PIT= Posterior Infero Temporal area; FST= Fundus of the Superior Temporal visual area; 6r = Rostral Area 6; V2= Second Visual Area. The symbol "*" indicates that there was no area corresponding to the coordinates according to the HCP surface parcellation, indicating the possibility that the area was located underneath the surface.

Supplementary Table 1). Indeed, the right LOC resulted to be significantly functionally connected with early visual areas like bilateral V1 and V2, with bilateral SPG in the parietal lobes including left and right areas of the PPC like MIP and LIP and areas as well as bilateral portions of the inferior parietal lobule (IPG). In the temporal lobes, bilateral ITG and MTG, with a consistent portion of overlapping activation in the right MT+ complex. Finally, rLOC showed significant functional co-activation with regions in the right and left frontal lobes; particularly in bilateral Supplementary Motor Area (SMA), bilateral Superior and Middle Frontal Gyri (SMG and MFG) and bilateral PreCG, including consistent overlapping activation in the right PMv. Moreover, only the right Insula was found to be functionally interacting with the seed region.

4. Discussion

4.1. A dynamic network subtending illusion processing and perceptual inference

The current study aimed at investigating the functional network of areas involved in the construction of illusory percepts arising from shape, geometrical and motion illusions. Specifically, we chose only to include illusory configurations in which the contextual visual cues elicited univocal illusory percepts, thus excluding bistable illusions, habituation effects and optical effects that required a change in visual perspective (e.g., reverse perspective illusion). By focusing on these types of illusions, it was possible to elicit the areas involved in top-down

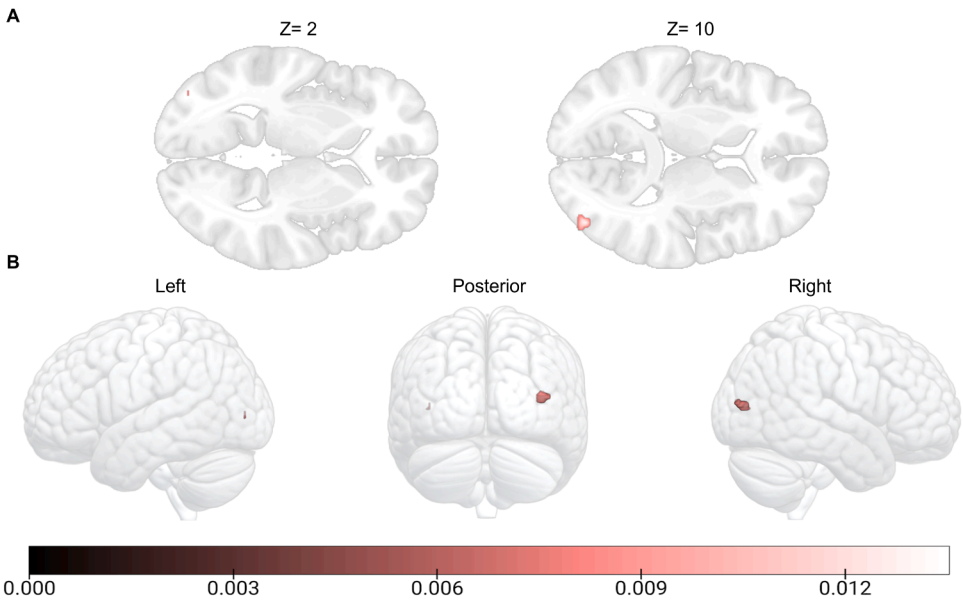

Fig. 6. Network of common activations resulting from the conjunction between the Static and Motion ALE networks [Static ∧ Motion]. **A.** The different clusters of overlapping activation are presented overlayed on the MNI152 volume template. MNI coordinates (Z) are provided for each slice. **B.** The same results are shown on a 3D rendered brain from different views: left hemisphere view, posterior view of both hemispheres and right hemisphere view. The color bar represents the increasing degree of convergence expressed by the ALE values.

Table 4
Results of the conjunction analysis between the two meta-analyses. For each cluster, the general brain region according to the AAL3 atlas and specific surface area according to the HCP parcellation are provided where possible. Hemisphere, cluster size (in mm^3) and ALE value are provided. MNI coordinates are reported for each peak present in the cluster.

ClusterStatic ∧ Motion	Region	Area	Hemisphere	Volume (mm^3)	ALE	Coordinates		
						x	y	z
Static ∧ Motion								
1	MOG	V3CD	RH	368	0.0135	42	-82	10
2	MOG	LO1	LH	32	0.0089	-40	-86	4

Notes. LH= Left Hemisphere; RH= Right Hemisphere. **Region labels**. MOG= Middle Occipital Gyrus. **Area labels**. LO1= Lateral Occipital 1.

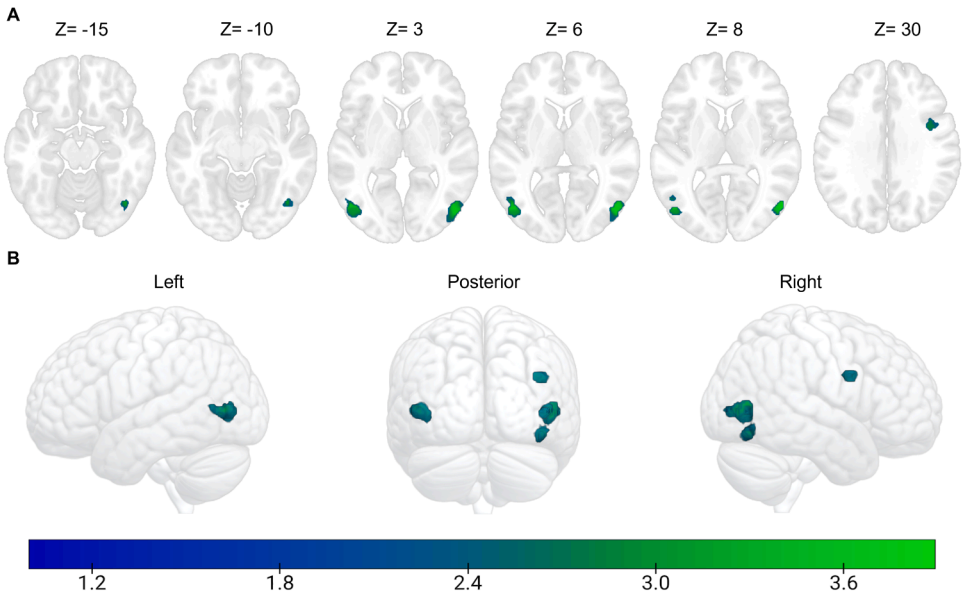

Fig. 7. Network of common activations resulting from the contrast between Motion and Static [Motion > Static] meta-analyses. **A.** The different clusters of overlapping activation are presented overlayed on the MNI152 volume template. MNI coordinates (Z) are provided for each slice. **B.** The same results are shown on a 3D rendered brain from different views: left hemisphere view, posterior view of both hemispheres and right hemisphere view. The color bar represents the increasing degree of convergence expressed by the ALE values.

processing underlying the construction of visual percepts and to investigate the degree to which the same areas are involved in building different perceptual features such as shape, length, depth and motion or whether these follow separated processing routes.

The results of the general meta-analysis, in which all types of illusions were pooled together, resulted in bilateral activations encompassing the middle and inferior occipital gyri. Specifically, the right-lateralized cluster of activation also encompassed the ITG and the FFG, while the left mainly extended across the inferior, middle and superior occipital gyri. Both the left and right MOG presented the highest degree of overlap as measured by the ALE value (see Table 2). Similarly, the two sub-metanalyses showed significant activations in analogous regions as confirmed by the conjunction analysis, in which only two small patches of overlapping activation emerged in the left and right

Table 5
Results of the contrast between Motion and Static [Motion > Static] meta-analyses. For each cluster, the general brain region according to the AAL3 atlas and specific surface area according to the HCP parcellation are provided where possible. Hemisphere, cluster size (in mm^3) and Z value are provided. MNI coordinates are reported for each peak present in the cluster.

Cluster	Region	Area	Hemisphere	Volume (mm^3)	Z	Coordinates		
						x	y	z
Motion > Static								
1	MTG	MT	RH	1864	3.719	52	-71.5	8.8
		V4t			3.719	49.1	-75.5	3.4
2	MOG	*	LH	1568	3.8906	-48.6	-72.7	5.7
3	PCG	IFJp	RH	608	2.9677	38.8	2	31.2
		6r			2.7703	42.5	5.1	28.2
		6r			2.3999	46	8	32
4	ITG	PH	RH	568	3.2905	46	-71	-12
	IOG	FFC			3.0115	42.7	-69.3	-15.3
	ITG	FST			2.4372	46	-66	-6
Static > Motion								
No suprathreshold clusters								

Notes. RH= Right Hemisphere; LH= Left Hemisphere. **Region labels**. MTG= Middle Temporal Gyrus; MOG= Middle Occipital Gyrus; PCG= Precentral Gyrus; ITG= Inferior Temporal Gyrus; IOG= Inferior Occipital Gyrus. **Area labels**. MT= Middle Temporal Area; 6r= Rostral Area 6; FFC= Fusiform Face Complex; FST= Fundus of the Superior Temporal visual area. The symbol "*" indicates that there was no area corresponding to the coordinates according to the HCP surface parcellation, indicating the possibility that the area was located underneath the surface.

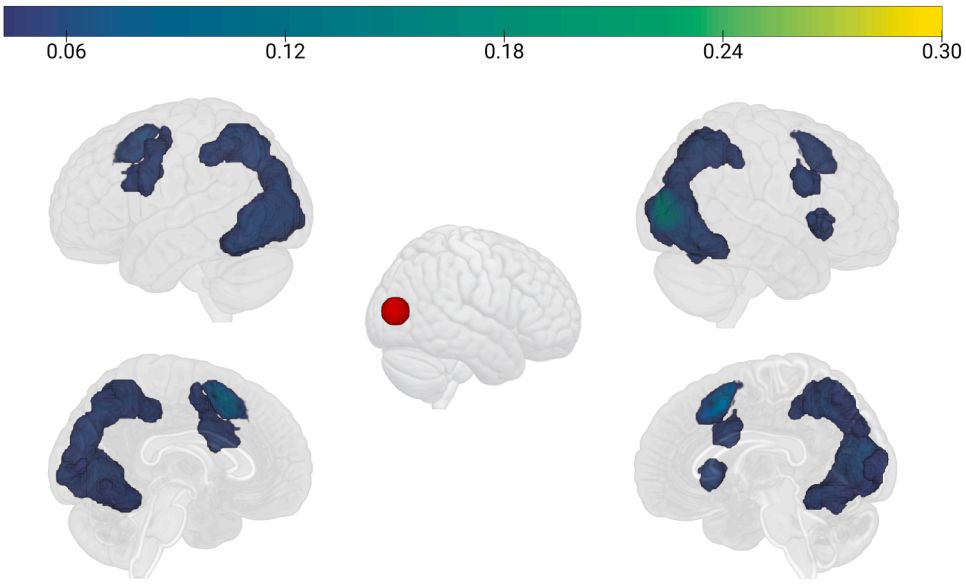

Fig. 8. Results of the MACM functional connectivity analysis representing the areas significantly co-activated with the right LOC. The image at the center shows the spherical ROI (12 mm) centered on the peak resulting from the conjunction analysis in the right hemisphere (MNI: 42, -82, 10). The left side of the figure displays areas functionally connected to this region in the left hemisphere; while the right side displays the functionally connected regions in the right hemisphere (upper side: lateral view; lower side: medial view).

MOG, centered in the right V3CD and the left LO1. These areas are part of the Lateral Occipital Complex (Table 2 in Cocuzza et al., 2022; Grill-Spector et al., 1998; Hasson et al., 2001; Levy et al., 2001; Malach et al., 1995), known to be involved in the global analysis of shape and in recognition (for a classic review see Grill-Spector et al. 2001). The current results confirm previous accounts demonstrating that the LOC region contributes to a variety of optical geometrical illusions (Brighina et al., 2003; Hirsch et al., 1995; Ritzl et al., 2003; Seghier et al., 2000; Tabei et al., 2015; Weidner et al., 2010; Weidner and Fink, 2007), and acts as a central node for both illusory and real contour completion (de-Wit et al., 2009; Huxlin et al., 2000; Mendola et al., 1999; Shpaner et al., 2009; Wokke et al., 2013), Müller-Lyer (Mancini et al., 2011; Vallar et al., 2000) and Ponzo (Zeng et al., 2020).

In the context of illusory contours, it has been proposed that the perceptual completion is driven from LOC to early visual areas V1/V2, with interactions between mid-level and lower-tier visual areas in the visual hierarchy engaging in object completion via recurrent processes (Stanley and Rubin, 2003). Chen and colleagues (2021) tested this by modeling the effective connectivity between LOC and early visual processing areas such as V1 and V2 using dynamic causal modeling, concluding that information processing is integrated across different levels of visual hierarchy by a combination of feedback and feedforward processing (Lee and Nguyen, 2001; Stanley and Rubin, 2003). They argue against the pure feedforward processing accounts, which, conversely, posit that visual processing moves hierarchically from early visual areas, where basic features are processed, to higher areas where more complex features are integrated in the percept (Ffytche and Zeki, 1996; Grosof et al., 1993; Leventhal et al., 1998; Sheth et al., 1996).

TMS evidence confirms this account given that early disruption in LOC degrades object completion performance while disruption in V1/V2 interferes with performance only later in the processing (Wokke et al., 2013). Indeed, while the present results show consistent overlapping activation in both left and right LOC, there is significantly less overlap in early visual areas, suggesting a primary role of higher order visual areas in building illusory percepts compared to areas lower in the hierarchy.

Lesser attention has been posed on the involvement of this area in the processing of illusory self-motion and motion-related illusions. Indeed, the LOC was previously described as being involved in the processing of kinetic boundaries (Dupont et al., 1997; Larsson and Heeger, 2006; Van Oostende et al., 1997), depth structure boundaries (Tyler et al., 2006) and second-order pattern perception (Larsson et al., 2006). Sulpizio and colleagues (2020) found portions of the LOC, including bilateral LO1

and V3CD, to be jointly activated by scene/place and egomotion stimuli, suggesting that these and other regions of the dorsolateral parieto-occipital cortex play a key role in extracting both complex visual patterns and high-order motion information. Hence, the present findings are in line with previous accounts and indicate that the LOC region is commonly activated during the generation of different types of percepts and may act as a central node in the ventral and dorsal dynamic interplay underlying perceptual integration.

Outside the occipital cortex, activation extended ventrally in the temporal lobe in the general meta-analysis and similarly in the static and motion illusions sub-meta-analyses. In the static illusions network, activity in the fusiform and lingual gyri peaked in V4, as identified by the HCP atlas. Indeed, previous non-human primates' findings demonstrated that neurons in this area selectively fire in response to Kanizsa surfaces (Cox et al., 2013) and lesions to this area result in impairments in perceiving illusory contours (De Weerd et al., 1996). Therefore, neurons in V4 are thought to be involved in representing geometric regularities and contextual information with the purpose of deriving a percept from the general image, thus distinguishing the object from the context (for an extensive review on the visual functions of primates' V4 see Pasupathy et al. 2020).

On the other hand, the motion ALE network extended even further along the areas of the ventral pathway compared to the static network (Fig. 9). Activation was detected in the MTG of both hemispheres reaching PIT in the right hemisphere and reaching the FST in the left hemisphere. This latter area was active together with V4t and MT which are all part of the MT+ complex and contribute differently to several aspects of motion perception such as object motion, coherent optic flow and increasing object velocities (Sulpizio et al., 2022; 2023). Outside the MT+ complex, the motion illusion network presented a cluster in the right SOG centered in V2, which was demonstrated to be functionally connected to MT+ complex (Sulpizio et al., 2022) and has been proposed to act as node devoted to updating spatial representations (Wolbers et al., 2008). Interestingly, no parietal common activation survived in the motion illusion network. Conversely, both the general and the static illusion ALE network comprehended a cluster of activation in the right SPG; specifically, in the Posterior Parietal Cortex (PPC) with peaks in VIP and MIP. In general, this region has been found to be involved in directing attention to either global or local aspects of complex figures (Ritzl et al., 2003; Wu et al., 2012) and the right PPC is well known to be involved in visuospatial processing by representing and transforming references frames (Andersen and Buneo, 2002) and in integrating multisensory information supporting action planning thanks to fronto-parietal feedback and feedforward interactions (Bencivenga and Tullo et al., 2023). In the context of illusions, the neuroimaging studies reviewed and analyzed here propose that the right SPC activity is modulated by illusion strength in response to Müller-Lyer (Plewan et al., 2012; Weidner and Fink, 2007), and is recruited during the presentation of Poggendorf illusion and Illusory contours (Shen et al., 2016), Roelofs (Walter and Dassonville, 2008) and Ebbinghaus illusions (Chen et al., 2022). However, its involvement in illusion processing has been proposed to be indirect: possibly integrating and updating size invariant representations and actively using illusion information for judgment and comparison after the illusion is formed, but not generating the illusion per se (Plewan et al., 2012; Kreutzer et al., 2015). Indeed, Mancini and colleagues (2011) applied rTMS to the left and right SPC and found no difference in perceiving the Müller-Lyer illusion in different modalities, while the stimulation of bilateral LOC did affect the illusion perception. Moreover, TMS interference over the Superior parietal lobule did not affect neither the global nor the local perception of a grouped illusory Gestalt stimulus; while disrupting anterior IPS activity resulted in a shortening of the Global percept (Zaretskaya et al., 2013). Overall, these findings support the view of an indirect contribution of SPC.

Fig. 9. Comparison of clusters of converging activation related to both the static illusions network (yellow) and the motion illusions network (blue) rendered on the same space. Regions in green represent areas in which the two networks overlapped.

Thus, the right SPC may act as a higher-level processing unit receiving information from LOC, which in turn supports the formation of the visual percept thanks to recurrent feedforward and feedback connections with V1 and V2 (Bullier, 2001; Chen et al., 2021; Stanley and Rubin, 2003). Similarly, motion related illusions are likely supported by an interaction between the dorsolateral parieto-occipital cortex with early visual areas (Sulpizio, 2020). Indeed, the [Motion > Static] contrast, representing the areas exclusively involved in motion perception, is very similar to the network emerging from the Motion illusion meta-analysis alone. The main difference between the two is that the latter lacks activations in LOC and early visual areas, confirming the role of these areas in computing the two classes of illusions. Converging activity specific to the processing of motion-related illusions emerged in the PreCG, including 6r and IFJp of the ventral Premotor Cortex. This region has been demonstrated not only to be involved in action preparation, but also in cognitive functions including space perception and action understanding, supported by multimodal convergence between tactile, moving visual stimuli and auditory stimuli (Rizzolatti and Craighero, 2004; Rizzolatti and Luppino, 2001). Jia and Colleagues (2018) found an increase forward effective connectivity from area V3A and PMv following training employing a motion discrimination task, reflecting an improvement in sensory accumulation process (Dosher et al., 2013; Dosher and Lu, 1998, 2005). Dynamic causal modeling results suggest strengthened feedforward connection from V3A to PMv, but not from MT+ to higher areas, in line with the critical role of V3A in refining sensory representation in motion perceptual learning. These results are supportive of the feature-based learning (Shibata et al., 2014; Watanabe and Sasaki, 2015).

Taken together, these results present a bilateral network of illusion processing distributed along ventral and dorsal areas, particularly extended in the right hemisphere. Our findings and the related evidence reviewed above are in line with previous accounts supporting a recurrent model of visual processing and conscious perception (Bullier, 2001; Lamme and Roelfsema, 2000) based on backward connections from higher order to lower visual areas. In contrast to the pure feedforward models, information from dorsal higher processing areas gets "retro-injected" in primary visual areas such as V1 and V2 that act as "active blackboards" for the other visual cortical areas. Neurons of V4, MT, LOC or PPC are characterized by larger receptive fields compared to the ones of lower regions' neurons; thus, allowing for the integration of global information and to "inform" earlier areas of such processing. Particularly, this is the basis of Bayesian perceptual inference accounts (Friston, 2005a) in which the backward connections from higher order visual areas provide contextual guidance to lower levels through the predictions of the lower level's inputs (i.e., the forward flow of information lower to higher order areas in the visual hierarchy). This conceptualization is particularly relevant for contextual illusions treated in the present study given the importance of global processing for the emergence of the illusory percept. Particularly, illusions represent where our perception reliably and indomitably disagrees with the true nature of the raw sensory information (Gregory, 1997). Therefore, illusory percepts do not represent failures in the perceptual apparatus; instead, they demonstrate how perceptual inference uses contextual information and

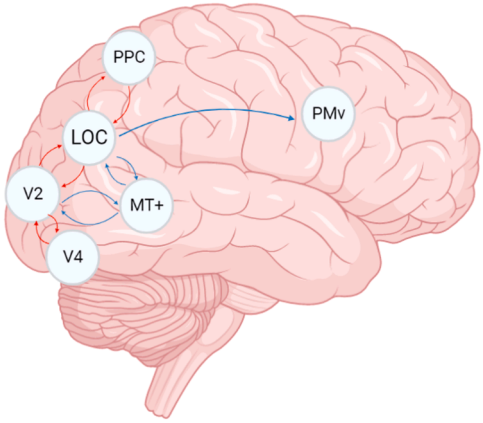

Fig. 10. Schematic representation of the possible forward and backward mechanisms underlying illusions processing based on reviewed evidence. Red lines represent processing related to static illusions while blue lines represent processing related to motion illusions.

prior assumptions to constrain interpretations of sensory data (Brown and Friston, 2012; Nour and Nour, 2015; Purves et al., 2011).

The proposed central role of LOC, particularly the right one, in integrating perceptual representations is confirmed by the functional connectivity network resulting from the MACM analysis, which suggests that this region is consistently functionally connected with the PPC, MT+ complex and PMv in the right hemisphere as well as the left LOC, its corresponding counterpart in the left hemisphere.

Fig. 10 summarizes the areas involved in perceptual inference underlying the two types of illusions and how they exchange forward and backward information based on previous theoretical and experimental accounts reviewed and supported by the MACM functional connectivity results.

4.2. Implications in the subdivision of ventral and dorsal processing pathways

As stated above, the current results present networks underlying perceptual inference distributed along both ventral and dorsal pathways independently of the type of the perceptual features elicited by the illusory configurations. The static illusions considered here include features such as size, length or shape that could have been expected to predominantly drive activity along ventral areas, following the perception-action model, but this is not the case. Similarly, motion illusions consistently recruit ventral areas even if they involve movement perception and illusory motion, depth and changes in direction, features that are all strictly linked to action preparation and classically ascribed exclusively to dorsal processing. Moreover, the present and the reviewed evidence indicate that both the ventral and dorsal visual pathways are modulated by illusion strength. Indeed, other accounts on the ventro-dorsal interactions, state that it is the visual attribute that determines whether the information will be processed in ventral or dorsal areas instead of whether the information is used for perception or action (de la Malla et al., 2019; Smeets et al., 2020; Smeets and Brenner, 2019), and that size illusions can be processed along both the ventral and the dorsal pathways, depending on which spatial attributes are used (Smeets et al., 2002); contrasting the predictions of the classical perception-action model. This evidence argues against an absolute distinction between ventral and dorsal streams and favors the view of the two pathways manifesting a strong interconnected network, sharing various processing characteristics (e.g., de Haan and Cowey 2011, Pavani et al. 1999).

4.3. Implications for illusion classification and schizophrenia

The present results show which areas are involved in the processing of different types of visual illusions and lay the foundation for a classification system of illusions based on the neural mechanisms from which they arise (Hamburger, 2016). Outside the illusion domain per se, the described networks show the regions that interact to support the feedback and feedforward loops underlying perceptual and sensory integration. In this regard, particular attention has been posed on the study of hallucinogenic symptoms following a hodotopic framework, in which visual and auditory aberrant phenomena are explained by hypo- or hyper-connectivity between cortical regions (Ffytche, 2008). In this context, schizophrenia symptoms are known to be characterized in marked differences in perceptual organization and integrative functions; thought to result from a large-scale dysconnectivity syndrome (Amad et al., 2014; Burns et al., 2003; Friston, 1998, 2005b; Frith and Done, 1988; Liang et al., 2006; Schmitt et al., 2011; Stephan et al., 2009). A recent systematic review on studies assessing schizophrenic patients' performance in perceiving different types of illusions (including geometrical illusions, illusory contours and motion illusions) found concordant evidence for an abnormal sensitivity of patients to most of the categories. Thus, suggesting that an impaired top-down process involved in depth perception constitutes a common perceptual feature in schizophrenia (Costa et al., 2023). As discussed above, visual illusions are clear examples that elicit how our inferential perceptual process works and can be explained as resulting from a recurrent interaction between feedforward and feedback loops between areas at different points in the processing hierarchy. Similarly, symptoms like delusions and hallucinations have been linked to a general disruption in the perceptual inferential process; resulting in false inferences given by an imbalance in the weight attributed to priors or to sensory evidence (Fletcher and Frith, 2009; Friston, 2005b; Schmack et al., 2013 for a clear and extensive review of the relationship between illusions and hallucinations explained by a bayesian framework see Notredame et al. 2014). Therefore, visual illusions and hallucinations may tap on analogous predictive perceptual mechanisms; the same that are likely to be impaired in schizophrenia, thus resulting in a reduced sensitivity to visual illusions. Understanding how patients respond to illusory percepts could also inform about the underlying perceptual processes that are impaired in the disorder (White and Shergill, 2012). To conclude, visual illusions may be considered as possible biomarkers for schizophrenia and most likely also for other pathologies characterized by the presence of hallucinations such as in degenerative Lewy body disease (D'Antonio et al., 2022) or Alzheimer's disease psychosis (D'Antonio, Di Vita, et al., 2022; D'Antonio et al., 2019) where the brain circuit underlying the perception of optical illusions might be impaired before the onset of hallucinations providing crucial indications for differential diagnosis.

5. Limitations

ALE coordinate-based meta-analyses are sensitive to the number experiments included in the analysis and it is recommended to have at least around 20 experiments to have meaningful statistical power (see Fig. 8 in Eickhoff et al., 2016). In the present study, the motion-illusions ALE included 13 experiments found in the literature, therefore care must be taken when interpreting the results. However, these experiments included a consistent number of foci (see Fig. 1, Table 1) and the resulting ALE networks are coherent with previous accounts on illusion processing and motion perception, as further supported by our MACM results. About the MACM, we chose to keep the task constraints less stringent as possible in order to have a compelling view of the connectivity of the rLOC which is independent of specific tasks or conditions. Thus, our results should be intended to reflect a general co-activation map of the rLOC, rather than specific (context-dependent) connectivity patterns depending on the task or condition at hand (e.g., motion-induced visual illusions).

6. Conclusions

Here, we defined a general network of areas that contribute to the formation of illusory percepts, laying the foundation for a neural classification of illusions. The comparison of the two networks is informative of the distinction between ventral and dorsal processing and argues against a strict division of labor argued by the perception-action model. The areas described here are involved in feedback and feedforward loops underlying visual perceptual processing and the networks in which they interact support the predictive mechanisms of the brain in integrating contextual information. The understanding of these mechanisms potentially has crucial implications in the investigation of biomarkers for schizophrenia research and for neurodegenerative disorders characterized by delusions.

Ethics statement

There were no ethical concerns on this study as no original data was directly acquired from the authors.

Data and code availability statement

All the data used for the analysis was extracted from the papers that met our a priori criteria (listed in Table 1) and processed using the freely available GingerALE 3.0.2 software (http://brainmap.org/ale). The processed data required to reproduce the above findings are available to download from: https://osf.io/p5d9f/ .

Funding

This research did not receive any specific grant from funding agencies in the public, commercial, or not-for-profit sectors.

Declaration of Competing Interest

None.

Supplementary materials

Supplementary material associated with this article can be found, in the online version, at doi:10.1016/j.neuroimage.2023.120335.

References

Aglioti, S., DeSouza, J.F.X., Goodale, M.A., 1995. Size-contrast illusions deceive the eye but not the hand. Curr. Biol. 5 (6), 679–685. https://doi.org/10.1016/S0960-9822(95)00133-3. Scopus.

Amad, A., Cachia, A., Gorwood, P., Pins, D., Delmaire, C., Rolland, B., Mondino, M., Thomas, P., Jardri, R., 2014. The multimodal connectivity of the hippocampal complex in auditory and visual hallucinations. Mol. Psychiatry 19 (2). https://doi.org/10.1038/mp.2012.181. Article 2.

Andersen, R.A., Buneo, C.A., 2002. Intentional maps in posterior parietal cortex. Annu. Rev. Neurosci. 25 (1), 189–220. https://doi.org/10.1146/annurev.neuro.25.112701.142922.

Bencivenga, F., Tullo, M.G., Maltempo, T., von Gal, A., Serra, C., Pitzalis, S., Galati, G., 2023. Effector-selective modulation of the effective connectivity within frontoparietal circuits during visuomotor tasks. Cereb. Cortex 33 (6), 2517–2538. https://doi.org/10.1093/cercor/bhac223.

Boring, E.G., 1942. Sensation and Perception in the History of Experimental Psychology. Appleton-Century pp. xv, 644.

Brighina, F., Ricci, R., Piazza, A., Scalia, S., Giglia, G., Fierro, B., 2003. Illusory contours and specific regions of human extrastriate cortex: evidence from rTMS. Eur. J. Neurosci. 17 (11), 2469–2474. https://doi.org/10.1046/j.1460-9568.2003.02679.x.

Brown, H., Friston, K., 2012. Free-energy and illusions: the Cornsweet effect. Front. Psychol. 3. https://www.frontiersin.org/articles/10.3389/fpsyg.2012.00043.

Bruno, N., Franz, V.H., 2009. When is grasping affected by the Müller-Lyer illusion? A quantitative review. Neuropsychologia 47 (6), 1421–1433. https://doi.org/10.1016/j.neuropsychologia.2008.10.031.

Budnik, U., Hindi-Attar, C., Hamburger, K., Pinna, B., Hennig, J., Speck, O., 2016. Perceptual experience of visual motion activates hMT+ independently from the physical reality: fMRI insights from the looming pinna figure. Perception 45 (11), 1211–1221. https://doi.org/10.1177/0301006616652051.

Bullier, J., 2001. Integrated model of visual processing. Brain Res. Brain Res. Rev. 36 (2–3), 96–107. https://doi.org/10.1016/s0165-0173(01)00085-6.

Burns, J., Job, D., Bastin, M.E., Whalley, H., Macgillivray, T., Johnstone, E.C., Lawrie, S. M., 2003. Structural disconnectivity in schizophrenia: a diffusion tensor magnetic resonance imaging study. Br. J. Psychiatry 182 (5), 439–443. https://doi.org/10.1192/bjp.182.5.439.

Chen, L., Zhu, S., Feng, B., Zhang, X., Jiang, Y., 2022. Altered effective connectivity between lateral occipital cortex and superior parietal lobule contributes to manipulability-related modulation of the Ebbinghaus illusion. Cortex 147, 194–205. https://doi.org/10.1016/j.cortex.2021.11.019.

Chen, S., Weidner, R., Zeng, H., Fink, G.R., Müller, H.J., Conci, M., 2021. Feedback from lateral occipital cortex to V1/V2 triggers object completion: evidence from functional magnetic resonance imaging and dynamic causal modeling. Hum. Brain Mapp. 42 (17), 5581–5594. https://doi.org/10.1002/hbm.25637.

Clark, A., 2013. Whatever next? Predictive brains, situated agents, and the future of cognitive science. Behav. Brain Sci. 36 (3), 181–204. https://doi.org/10.1017/S0140525x12000477. Cambridge Core.

Cocuzza, C. V., Ruben, S.R., Ito, T., Mill, R. D., Keane, B. P., & Cole, M. W. (2022). Distributed resting-state network interactions linked to the generation of local visual category selectivity. BioRxiv, 2022.02.19.481103. 10.1101/2022.02.19.481103.

Coello, Y., Danckert, J., Blangero, A., Rossetti, Y., 2007. Do visual illusions probe the visual brain? Illusions in action without a dorsal visual stream. Neuropsychologia 45 (8), 1849–1858. https://doi.org/10.1016/j.neuropsychologia.2006.12.010.

Coren, S., Girgus, J.S., Erlichman, H., Hakstian, A.R., 1976. An empirical taxonomy of visual illusions. Percept. Psychophys. 20, 129–137. https://doi.org/10.3758/BF03199444.

Costa, A.L.L., Costa, D.L., Pessoa, V.F., Caixeta, F.V., Maior, R.S., 2023. Systematic review of visual illusions in schizophrenia. Schizophr. Res. 252, 13–22. https://doi.org/10.1016/j.schres.2022.12.030.

Cox, M.A., Schmid, M.C., Peters, A.J., Saunders, R.C., Leopold, D.A., Maier, A., 2013. Receptive field focus of visual area V4 neurons determines responses to illusory surfaces. Proc. Natl. Acad. Sci. USA 110 (42), 17095–17100. https://doi.org/10.1073/pnas.1310806110.

D'Antonio, F., Boccia, M., Di Vita, A., Suppa, A., Fabbrini, A., Canevelli, M., Caramia, F., Fiorelli, M., Guariglia, C., Ferracuti, S., de Lena, C., Aarsland, D., Ffytche, D., 2022. Visual hallucinations in Lewy body disease: pathophysiological insights from phenomenology. J. Neurol. 269 (7), 3636–3652. https://doi.org/10.1007/s00415-022-10983-6.

D'Antonio, F., Di Vita, A., Zazzaro, G., Brusà, E., Trebbastoni, A., Campanelli, A., Ferracuti, S., Lena, C., Guariglia, C., Boccia, M., 2019. Psychosis of Alzheimer's disease: neuropsychological and neuroimaging longitudinal study. Int. J. Geriatr. Psychiatry 34 (11), 1689–1697. https://doi.org/10.1002/gps.5183.

D'Antonio, F., Di Vita, A., Zazzaro, G., Canevelli, M., Trebbastoni, A., Campanelli, A., Ferracuti, S., de Lena, C., Guariglia, C., Boccia, M., 2022. Cortical complexity alterations in the medial temporal lobe are associated with Alzheimer's disease psychosis. Aging Neuropsychol. Cogn. 29 (6), 1022–1032. https://doi.org/10.1080/13825585.2021.1958139.

de Haan, E.H.F., Cowey, A., 2011. On the usefulness of 'what' and 'where' pathways in vision. Trends Cogn. Sci. 15 (10), 460–466. https://doi.org/10.1016/j.tics.2011.08.005. Scopus.

de la Malla, C., Brenner, E., de Haan, E.H.F., Smeets, J.B.J., 2019. A visual illusion that influences perception and action through the dorsal pathway. Commun. Biol. 2, 38. https://doi.org/10.1038/s42003-019-0293-x.

de la Malla, C., Smeets, J.B.J., Brenner, E., 2018. Errors in interception can be predicted from errors in perception. Cortex 98, 49–59. https://doi.org/10.1016/j.cortex.2017.03.006.

De Weerd, P., Desimone, R., Ungerleider, L.G., 1996. Cue-dependent deficits in grating orientation discrimination after V4 lesions in macaques. Vis. Neurosci. 13 (3), 529–538. https://doi.org/10.1017/s0952523800008208.

de-Wit, L.H., Kentridge, R.W., Milner, A.D., 2009. Shape processing area LO and illusory contours. Perception 38 (8), 1260–1263. https://doi.org/10.1068/p6388. Vol. IssueSAGE PUBLICATIONS LTD.

Dosher, B.A., Jeter, P., Liu, J., Lu, Z.L., 2013. An integrated reweighting theory of perceptual learning. Proc. Natl. Acad. Sci. 110 (33), 13678–13683. https://doi.org/10.1073/pnas.1312552110.

Dosher, B.A., Lu, Z.L., 1998. Perceptual learning reflects external noise filtering and internal noise reduction through channel reweighting. Proc. Natl. Acad. Sci. USA 95 (23), 13988–13993.

Dosher, B.A., Lu, Z.L., 2005. Perceptual learning in clear displays optimizes perceptual expertise: learning the limiting process. Proc. Natl. Acad. Sci. 102 (14), 5286–5290. https://doi.org/10.1073/pnas.0500492102.

Dupont, P., De Bruyn, B., Vandenberghe, R., Rosier, A.M., Michiels, J., Marchal, G., Mortelmans, L., Orban, G.A., 1997. The kinetic occipital region in human visual cortex. Cereb. Cortex 7 (3), 283–292. https://doi.org/10.1093/cercor/7.3.283 (New York, N.Y.: 1991).

Eagleman, D.M., 2001. Visual illusions and neurobiology. Nat. Rev. Neurosci. 2 (12), 920–926. https://doi.org/10.1038/35104092.

Eickhoff, S.B., Bzdok, D., Laird, A.R., Kurth, F., Fox, P.T., 2012. Activation likelihood estimation meta-analysis revisited. Neuroimage 59 (3), 2349–2361. https://doi.org/10.1016/j.neuroimage.2011.09.017.

Eickhoff, S.B., Bzdok, D., Laird, A.R., Roski, C., Caspers, S., Zilles, K., Fox, P.T., 2011. Co-activation patterns distinguish cortical modules, their connectivity and functional differentiation. Neuroimage 57 (3), 938–949. https://doi.org/10.1016/j.neuroimage.2011.05.021.

Eickhoff, S.B., Laird, A.R., Grefkes, C., Wang, L.E., Zilles, K., Fox, P.T., 2009. Coordinate-based activation likelihood estimation meta-analysis of neuroimaging data: a

random-effects approach based on empirical estimates of spatial uncertainty. Hum. Brain Mapp. 30 (9), 2907–2926. https://doi.org/10.1002/hbm.20718.
Eickhoff, S.B., Nichols, T.E., Laird, A.R., Hoffstaedter, F., Amunts, K., Fox, P.T., Bzdok, D., Eickhoff, C.R., 2016. Behavior, sensitivity, and power of activation likelihood estimation characterized by massive empirical simulation. Neuroimage 137, 70–85. https://doi.org/10.1016/j.neuroimage.2016.04.072.
Ffytche, D.H., 2008. The hodology of hallucinations. Cortex 44 (8), 1067–1083. https://doi.org/10.1016/j.cortex.2008.04.005.
Ffytche, D.H., Zeki, S., 1996. Brain activity related to the perception of illusory contours. Neuroimage 3 (2), 104–108. https://doi.org/10.1006/nimg.1996.0012.
Fletcher, P.C., Frith, C.D., 2009. Perceiving is believing: a Bayesian approach to explaining the positive symptoms of schizophrenia. Nat. Rev. Neurosci. 10 (1), 48–58. https://doi.org/10.1038/nrn2536.
Fraedrich, E.M., Glasauer, S., Flanagin, V.L., 2010. Spatiotemporal phase-scrambling increases visual cortex activity. Neuroreport 21 (8), 596–600. https://doi.org/10.1097/WNR.0b013e32833a7e2f.
Franz, V.H., Gegenfurtner, K.R., Bülthoff, H.H., Fahle, M., 2000. Grasping visual illusions: no evidence for a dissociation between perception and action. Psychol. Sci. 11 (1), 20–25. https://doi.org/10.1111/1467-9280.00209. Scopus.
Friston, K.J., 1998. The disconnection hypothesis. Schizophr. Res. 30 (2), 115–125, 10.1016/s0920-9964(97)00140-0.
Friston, K.J., 2005a. A theory of cortical responses. Philos. Trans. Royal Soc. B Biol. Sci. 360 (1456), 815–836. https://doi.org/10.1098/rstb.2005.1622.
Friston, K.J., 2005b. Hallucinations and perceptual inference. Behav. Brain Sci. 28 (6), 764–766. https://doi.org/10.1017/S0140525x05290131.
Frith, C.D., Done, D.J., 1988. Towards a neuropsychology of schizophrenia. Br. J. Psychiatry J. Ment. Sci. 153, 437–443. https://doi.org/10.1192/bjp.153.4.437.
Galletti, C., Fattori, P., 2018. The dorsal visual stream revisited: stable circuits or dynamic pathways? Cortex 98, 203–217. https://doi.org/10.1016/j.cortex.2017.01.009.
Gallivan, J.P., Cant, J.S., Goodale, M.A., Flanagan, J.R., 2014. Representation of object weight in human ventral visual cortex. Curr. Biol. 24 (16), 1866–1873. https://doi.org/10.1016/j.cub.2014.06.046.
Glasser, M.F., Coalson, T.S., Robinson, E.C., Hacker, C.D., Harwell, J., Yacoub, E., Ugurbil, K., Andersson, J., Beckmann, C.F., Jenkinson, M., Smith, S.M., Van Essen, D. C., 2016. A multi-modal parcellation of human cerebral cortex. Nature 536 (7615). https://doi.org/10.1038/nature18933. Article 7615.
Goodale, M.A., Meenan, J.P., Bülthoff, H.H., Nicolle, D.A., Murphy, K.J., Racicot, C.I., 1994. Separate neural pathways for the visual analysis of object shape in perception and prehension. Curr. Biol. CB 4 (7), 604–610. https://doi.org/10.1016/s0960-9822(00)00132-9.
Goodale, M.A., Milner, A.D., 1992. Separate visual pathways for perception and action. Trends Neurosci. 15 (1), 20–25. https://doi.org/10.1016/0166-2236(92)90344-8.
Gregory, R.L., 1997. Visual illusions classified. Trends Cogn. Sci. 1 (5), 190–194. https://doi.org/10.1016/S1364-6613(97)01060-7.
Grill-Spector, K., Kourtzi, Z., Kanwisher, N., 2001. The lateral occipital complex and its role in object recognition. Vis. Res. 41 (10–11), 1409–1422. https://doi.org/10.1016/S0042-6989(01)00073-6.
Grill-Spector, K., Kushnir, T., Hendler, T., Edelman, S., Itzchak, Y., Malach, R., 1998. A sequence of object-processing stages revealed by fMRI in the human occipital lobe. Hum. Brain Mapp. 6 (4), 316–328, 10.1002/(SICI)1097-0193(1998)6:4<316::AID-HBM9>3.0.CO;2-6.
Grosof, D.H., Shapley, R.M., Hawken, M.J., 1993. Macaque VI neurons can signal 'illusory' contours. Nature 365 (6446). https://doi.org/10.1038/365550a0. Article 6446.
Hamburger, K., 2016. Visual illusions based on processes: new classification system needed. Perception 45 (5), 588–595. https://doi.org/10.1177/0301006616629038. Vol.IssueSAGE PUBLICATIONS LTD.
Hamm, J.P., Crawford, T.J., Nebl, H., Kean, M., Williams, S.C.R., Ettinger, U., 2014. Neural correlates of illusory line motion. PLoS ONE 9 (1), e87595. https://doi.org/10.1371/journal.pone.0087595.
Hasson, U., Hendler, T., Ben Bashat, D., Malach, R., 2001. Vase or face? A neural correlate of shape-selective grouping processes in the human brain. J. Cogn. Neurosci. 13, 744–753. https://doi.org/10.1162/08989290152541412.
Heywood, C.A., Cowey, A., Newcombe, F., 1991. Chromatic discrimination in a cortically colour blind observer. Eur. J. Neurosci. 3 (8), 802–812. https://doi.org/10.1111/j.1460-9568.1991.tb01676.x.
Hirsch, J., DeLaPaz, R.L., Relkin, N.R., Victor, J., Kim, K., Li, T., Borden, P., Rubin, N., Shapley, R., 1995. Illusory contours activate specific regions in human visual cortex: evidence from functional magnetic resonance imaging. Proc. Natl. Acad. Sci. USA 92 (14), 6469–6473. https://doi.org/10.1073/pnas.92.14.6469.
Huxlin, K.R., Saunders, R.C., Marchionini, D., Pham, H.A., Merigan, W.H., 2000. Perceptual deficits after lesions of inferotemporal cortex in macaques. Cereb. Cortex 10 (7), 671–683. https://doi.org/10.1093/cercor/10.7.671.
Jia, K., Xue, X., Lee, J.H., Fang, F., Zhang, J., Li, S., 2018. Visual perceptual learning modulates decision network in the human brain: the evidence from psychophysics, modeling, and functional magnetic resonance imaging. J. Vis. 18 (12), 9. https://doi.org/10.1167/18.12.9.
Koenderink, J., 2017. Visual illusions. *The Oxford compendium of visual illusions*, pp. 119–138.
Kovacs, G., Raabe, M., Greenlee, M., 2008. Neural correlates of visually induced self-motion illusion in depth. Cereb. Cortex 18 (8), 1779–1787. https://doi.org/10.1093/cercor/bhm203.
Kreutzer, S., Weidner, R., Fink, G.R., 2015. Rescaling retinal size into perceived size: evidence for an occipital and parietal bottleneck. J. Cogn. Neurosci. 27 (7), 1334–1343. https://doi.org/10.1162/jocn_a_00784.
Laird, A.R., Eickhoff, S.B., Kurth, F., Fox, P.M., Uecker, A.M., Turner, J.A., Robinson, J.L., Lancaster, J.L., Fox, P.T., 2009. ALE meta-analysis workfl ows via the BrainMap database: progress towards a probabilistic functional brain atlas. Front. Neuroinform. 3. https://doi.org/10.3389/neuro.11.023.2009. JUL.
Laird, A.R., Eickhoff, S.B., Rottschy, C., Bzdok, D., Ray, K.L., Fox, P.T., 2013. Networks of task co-activations. Neuroimage 80, 505–514. https://doi.org/10.1016/j.neuroimage.2013.04.073.
Lamme, V.A.F., Roelfsema, P.R., 2000. The distinct modes of vision offered by feedforward and recurrent processing. Trends Neurosci. 23 (11), 571–579. https://doi.org/10.1016/S0166-2236(00)01657-X.
Larsson, J., Heeger, D.J., 2006. Two retinotopic visual areas in human lateral occipital cortex. J. Neurosci. 26 (51), 13128–13142. https://doi.org/10.1523/JNEUROSCI.1657-06.2006.
Larsson, J., Landy, M.S., Heeger, D.J., 2006. Orientation-selective adaptation to first- and second-order patterns in human visual cortex. J. Neurophysiol. 95 (2), 862–881. https://doi.org/10.1152/jn.00668.2005.
Lee, T.S., Nguyen, M., 2001. Dynamics of subjective contour formation in the early visual cortex. Proc. Natl. Acad. Sci. 98 (4), 1907–1911. https://doi.org/10.1073/pnas.98.4.1907.
Leventhal, A.G., Wang, Y., Schmolesky, M.T., Zhou, Y., 1998. Neural correlates of boundary perception. Vis. Neurosci. 15 (6), 1107–1118. https://doi.org/10.1017/S0952523898156110.
Levy, I., Hasson, U., Avidan, G., Hendler, T., Malach, R., 2001. Center–periphery organization of human object areas. Nat. Neurosci. 4 (5) https://doi.org/10.1038/87490. Article 5.
Liang, M., Zhou, Y., Jiang, T., Liu, Z., Tian, L., Liu, H., Hao, Y., 2006. Widespread functional disconnectivity in schizophrenia with resting-state functional magnetic resonance imaging. Neuroreport 17 (2), 209–213. https://doi.org/10.1097/01.wnr.0000198434.06518.b8.
Malach, R., Reppas, J.B., Benson, R.R., Kwong, K.K., Jiang, H., Kennedy, W.A., Ledden, P. J., Brady, T.J., Rosen, B.R., Tootell, R.B., 1995. Object-related activity revealed by functional magnetic resonance imaging in human occipital cortex. Proc. Natl. Acad. Sci. USA 92, 8135–8139. https://doi.org/10.1073/pnas.92.18.8135.
Mancini, F., Bolognini, N., Bricolo, E., Vallar, G., 2011. Cross-modal processing in the occipito-temporal cortex: a TMS study of the Müller-Lyer illusion. J. Cogn. Neurosci. 23 (8), 1987–1997. https://doi.org/10.1162/jocn.2010.21561.
Medendorp, W.P., de Brouwer, A.J., Smeets, J.B.J., 2018. Dynamic representations of visual space for perception and action. Cortex 98, 194–202. https://doi.org/10.1016/j.cortex.2016.11.013.
Mendola, J.D., Dale, A.M., Fischl, B., Liu, A.K., Tootell, R.B.H., 1999. The representation of illusory and real contours in human cortical visual areas revealed by functional magnetic resonance imaging. J. Neurosci. 19 (19), 8560–8572.
Men'shikova, G., 2012. On the classification of visual illusions. Psikhologicheskie Issledovaniya 5, 1–16.
Milner, A.D., Goodale, M.A., 1995. The Visual Brain in Action. Oxford University Press (pp. xvii, 248).
Milner, A.D., Goodale, M.A., 2006. The Visual Brain in Action, 2nd ed. Oxford University Press. https://doi.org/10.1093/acprof:oso/9780198524724.001.0001. xxii, 297.
Milner, A.D., Goodale, M.A., 2008. Two visual systems re-viewed. Neuropsychologia 46 (3), 774–785. https://doi.org/10.1016/j.neuropsychologia.2007.10.005. Scopus.
Mishkin, M., Ungerleider, L.G., Macko, K.A., 1983. Object vision and spatial vision: two cortical pathways. Trends Neurosci. 6, 414–417. https://doi.org/10.1016/0166-2236(83)90190-X.
Murray, M., Wylie, G., Higgins, B., Javitt, D., Schroeder, C., Foxe, J., 2002. The spatiotemporal dynamics of illusory contour processing: combined high-density electrical mapping, source analysis, and functional magnetic resonance imaging. J. Neurosci. 22 (12), 5055–5073. https://doi.org/10.1523/JNEUROSCI.22-12-05055.2002.
Notredame, C.E., Pins, D., Deneve, S., Jardri, R., 2014. What visual illusions teach us about schizophrenia. Front. Integr. Neurosci. 8 https://doi.org/10.3389/fnint.2014.00063.
Nour, M.M., Nour, J.M., 2015. Perception, illusions and Bayesian inference. Psychopathology 48 (4), 217–221. https://doi.org/10.1159/000437271.
O'Reilly, J.X., Jbabdi, S., Behrens, T.E.J., 2012. How can a Bayesian approach inform neuroscience? Eur. J. Neurosci. 35 (7), 1169–1179. https://doi.org/10.1111/j.1460-9568.2012.08010.x. Scopus.
Page, M.J., McKenzie, J.E., Bossuyt, P.M., Boutron, I., Hoffmann, T.C., Mulrow, C.D., Shamseer, L., Tetzlaff, J.M., Akl, E.A., Brennan, S.E., Chou, R., Glanville, J., Grimshaw, J.M., Hróbjartsson, A., Lalu, M.M., Li, T., Loder, E.W., Mayo-Wilson, E., McDonald, S., Moher, D., 2021. The PRISMA 2020 statement: an updated guideline for reporting systematic reviews. BMJ 372. https://doi.org/10.1136/bmj.n71 n71.
Pasupathy, A., Popovkina, D.V., Kim, T., 2020. Visual functions of primate area V4. Annu. Rev. Vis. Sci. 6 (1), 363–385. https://doi.org/10.1146/annurev-vision-030320-041306.
Pavani, F., Boscagli, I., Benvenuti, F., Rabuffetti, M., Farnè, A., 1999. Are perception and action affected differently by the Titchener circles illusion? Exp. Brain Res. 127 (1), 95–101. https://doi.org/10.1007/s002210050777. Scopus.
Plewan, T., Weidner, R., Eickhoff, S.B., Fink, G.R., 2012. Ventral and dorsal stream interactions during the perception of the Müller-Lyer illusion: evidence derived from fMRI and dynamic causal modeling. J. Cogn. Neurosci. 24 (10), 2015–2029. https://doi.org/10.1162/jocn_a_00258.
Purves, D., Wojtach, W.T., Beau Lotto, R., 2017. 9 why the concept of "Visual Illusions" is misleading. In A. G. Shapiro & D. Todorovic (Eds.). The Oxford Compendium of Visual Illusions. Oxford University Press. https://doi.org/10.1093/acprof:oso/9780199794607.003.0009, p. 0.

Purves, D., Wojtach, W.T., Lotto, R.B., 2011. Understanding vision in wholly empirical terms. Proc. Natl. Acad. Sci. 108 (supplement_3), 15588–15595. https://doi.org/10.1073/pnas.1012178108.
Riedel, E., Stephan, T., Deutschländer, A., Kalla, R., Wiesmann, M., Dieterich, M., Brandt, T., 2005. Imaging the visual autokinetic illusion with fMRI. Neuroimage 27 (1), 163–166. https://doi.org/10.1016/j.neuroimage.2005.03.029.
Ritzl, A., Marshall, J., Weiss, P., Zafiris, O., Shah, N., Zilles, K., Fink, G., 2003. Functional anatomy and differential time courses of neural processing for explicit, inferred, and illusory contours–an event-related fMRI study. Neuroimage 19 (4), 1567–1577. https://doi.org/10.1016/S1053-8119(03)00180-0.
Rizzolatti, G., Craighero, L., 2004. The mirror-neuron system. Annu. Rev. Neurosci. 27 (1), 169–192. https://doi.org/10.1146/annurev.neuro.27.070203.144230.
Rizzolatti, G., Luppino, G., 2001. The cortical motor system. Neuron 31 (6), 889–901. https://doi.org/10.1016/S0896-6273(01)00423-8.
Robinson, J.L., Laird, A.R., Glahn, D.C., Lovallo, W.R., Fox, P.T., 2009. Metaanalytic connectivity modeling: delineating the functional connectivity of the human amygdala. Hum. Brain Mapp. 31 (2), 173–184. https://doi.org/10.1002/hbm.20854.
Rogers, B., 2022. When is an illusion not an illusion? An alternative view of the illusion concept. Front. Hum. Neurosci. 16, 957740 https://doi.org/10.3389/fnhum.2022.957740.
Rolls, E.T., Huang, C.C., Lin, C.P., Feng, J., Joliot, M., 2020. Automated anatomical labelling atlas 3. Neuroimage 206, 116189. https://doi.org/10.1016/j.neuroimage.2019.116189.
Schmack, K., Sekutowicz, M., Rössler, H., Brandl, E.J., Müller, D.J., Sterzer, P., 2013. The influence of dopamine-related genes on perceptual stability. Eur. J. Neurosci. 38 (9), 3378–3383. https://doi.org/10.1111/ejn.12339.
Schmitt, A., Hasan, A., Gruber, O., Falkai, P., 2011. Schizophrenia as a disorder of disconnectivity. Eur. Arch. Psychiatry Clin. Neurosci. 261 (Suppl 2), S150–S154. https://doi.org/10.1007/s00406-011-0242-2. Suppl 2.
Seghier, M., Dojat, M., Delon-Martin, C., Rubin, C., Warnking, J., Segebarth, C., Bullier, J., 2000. Moving illusory contours activate primary visual cortex: an fMRI study. Cereb. Cortex 10, 663–670. https://doi.org/10.1093/cercor/10.7.663. Vol. Issue 7OXFORD UNIV PRESS INC.
Shapiro, A.G., Todorovic, D., 2017. XIX Introduction. The Oxford Compendium of Visual Illusions. Oxford University Press. https://doi.org/10.1093/acprof:oso/9780199794607.002.0007, p. 0.
Shen, L., Zhang, M., Chen, Q., 2016. The Poggendorff illusion driven by real and illusory contour: behavioral and neural mechanisms. Neuropsychologia 85, 24–34. https://doi.org/10.1016/j.neuropsychologia.2016.03.005.
Sheth, B.R., Sharma, J., Rao, S.C., Sur, M., 1996. Orientation maps of subjective contours in visual cortex. Science 274 (5295), 2110–2115. https://doi.org/10.1126/science.274.5295.2110.
Shibata, K., Sagi, D., Watanabe, T., 2014. Two-stage model in perceptual learning: toward a unified theory. Ann. NY Acad. Sci. 1316 (1), 18–28. https://doi.org/10.1111/nyas.12419.
Shpaner, M., Murray, M.M., Foxe, J.J., 2009. Early processing in the human lateral occipital complex is highly responsive to illusory contours but not to salient regions. Eur. J. Neurosci. 30 (10), 2018–2028. https://doi.org/10.1111/j.1460-9568.2009.06981.x.
Smeets, J.B.J., Brenner, E., 2019. Some illusions are more inconsistent than others. Perception 48 (7), 638–641. https://doi.org/10.1177/0301006619853147.
Smeets, J.B.J., Brenner, E., de Grave, D.D.J., Cuijpers, R.H., 2002. Illusions in action: consequences of inconsistent processing of spatial attributes. Exp. Brain Res. 147 (2), 135–144. https://doi.org/10.1007/s00221-002-1185-7.
Smeets, J.B.J., Kleijn, E., van der Meijden, M., Brenner, E., 2020. Why some size illusions affect grip aperture. Exp. Brain Res. 238 (4), 969–979. https://doi.org/10.1007/s00221-020-05775-1.
Spillmann, L., 2009. Phenomenology and neurophysiological correlations: two approaches to perception research. Vis. Res. 49 (12), 1507–1521. https://doi.org/10.1016/j.visres.2009.02.022.
Stanley, D.A., Rubin, N., 2003. fMRI activation in response to illusory contours and salient regions in the human lateral occipital complex. Neuron 37 (2), 323–331. https://doi.org/10.1016/S0896-6273(02)01148-0.
Stephan, K.E., Friston, K.J., Frith, C.D., 2009. Dysconnection in schizophrenia: from abnormal synaptic plasticity to failures of self-monitoring. Schizophr. Bull. 35 (3), 509–527. https://doi.org/10.1093/schbul/sbn176.
Sulpizio, V., Galati, G., Fattori, P., Galletti, C., Pitzalis, S., 2020. A common neural substrate for processing scenes and egomotion-compatible visual motion. Brain Struct. Funct. 225 (7), 2091–2110. https://doi.org/10.1007/s00429-020-02112-8.
Sulpizio, V., von Gal A., Galati G., Fattori P., Galletti C., Pitzalis S., 2023. Neural sensitivity to translation self- and object-motion velocities. Manuscript submitted for publication.
Sulpizio, V., Strappini, F., Fattori, P., Galati, G., Galletti, C., Pecchinenda, A., Pitzalis, S., 2022. The human middle temporal cortex responds to both active leg movements and egomotion-compatible visual motion. Brain Struct. Funct. 227 (8), 2573–2592. https://doi.org/10.1007/s00429-022-02549-z.
Tabei, K.I., Satoh, M., Kida, H., Kizaki, M., Sakuma, H., Sakuma, H., Tomimoto, H., 2015. Involvement of the extrageniculate system in the perception of optical illusions: a functional magnetic resonance imaging study. PLoS ONE 10 (6), e0128750. https://doi.org/10.1371/journal.pone.0128750.
Tanaka, R., Yotsumoto, Y., 2016. Networks extending across dorsal and ventral visual pathways correlate with trajectory perception. J. Vis. 16 (6) https://doi.org/10.1167/16.6.21. Vol.IssueASSOC RESEARCH VISION OPHTHALMOLOGY INC.
Todorović, D., 2020. What are visual illusions? Perception 49 (11), 1128–1199. https://doi.org/10.1177/0301006620962279.
Turkeltaub, P.E., Eden, G.F., Jones, K.M., Zeffiro, T.A., 2002. Meta-analysis of the functional neuroanatomy of single-word reading: method and validation. Neuroimage 16, 765–780. https://doi.org/10.1006/nimg.2002.1131, 3 I.
Tyler, C., Likova, L., Kontsevich, L., Wade, A., 2006. The specificity of cortical region KO to depth structure. Neuroimage 30 (1), 228–238. https://doi.org/10.1016/j.neuroimage.2005.09.067.
Ungerleider, L.G., 1982. Two cortical visual systems. Analysis of Visual Behavior, p. 549. Chapter-18.
Vallar, G., Daini, R., Antonucci, G., 2000. Processing of illusion of length in spatial hemineglect: a study of line bisection. Neuropsychologia 38 (7), 1087–1097. https://doi.org/10.1016/S0028-3932(99)00139-6.
van der Hoorn, A., Beudel, M., de Jong, B.M., 2010. Interruption of visually perceived forward motion in depth evokes a cortical activation shift from spatial to intentional motor regions. Brain Res. 1358, 160–171. https://doi.org/10.1016/j.brainres.2010.08.050.
Van Oostende, S., Sunaert, S., Van Hecke, P., Marchal, G., Orban, G.A., 1997. The kinetic occipital (KO) region in man: an fMRI study. Cereb. Cortex 7 (7), 690–701. https://doi.org/10.1093/cercor/7.7.690.
Vicario, G.B., 2011. In: Illusioni ottico- geometriche: una rassegna di problemi. Istituto Veneto di Scienze, Lettere ed Arti, Venezia, Italy.
Wade, N.J., 2017. Early history of illusions. The Oxford Compendium of Visual Illusions. Oxford University Press, pp. 3–37.
Walter, E., Dassonville, P., 2008. Visuospatial contextual processing in the parietal cortex: an fMRI investigation of the induced Roelofs effect. Neuroimage 42 (4), 1686–1697. https://doi.org/10.1016/j.neuroimage.2008.06.016.
Watanabe, T., Sasaki, Y., 2015. Perceptual learning: toward a comprehensive theory. Annu. Rev. Psychol. 66 (1), 197–221. https://doi.org/10.1146/annurev-psych-010814-015214.
Weidner, R., Boers, F., Mathiak, K., Dammers, J., Fink, G.R., 2010. The temporal dynamics of the Müller-Lyer illusion. Cereb. Cortex 20, 1586–1595. https://doi.org/10.1093/cercor/bhp217.
Weidner, R., Fink, G.R., 2007. The neural mechanisms underlying the Müller-Lyer illusion and its interaction with visuospatial judgments. Cereb. Cortex 17 (4), 878–884. https://doi.org/10.1093/cercor/bhk042.
Weidner, R., Plewan, T., Chen, Q., Buchner, A., Weiss, P., Fink, G., 2014. The moon illusion and size-distance scaling-evidence for shared neural patterns. J. Cogn. Neurosci. 26 (8), 1871–1882. https://doi.org/10.1162/jocn_a_00590.
Westheimer, G., 2008. Illusions in the spatial sense of the eye: geometrical–optical illusions and the neural representation of space. Vis. Res. Rev. 48 (20), 2128–2142. https://doi.org/10.1016/j.visres.2008.05.016.
White, T.P., Shergill, S.S., 2012. Using illusions to understand delusions. Front. Psychol. 3, 407. https://doi.org/10.3389/fpsyg.2012.00407.
Wokke, M.E., Vandenbroucke, A.R.E., Scholte, H.S., Lamme, V.A.F., 2013. Confuse your illusion: feedback to early visual cortex contributes to perceptual completion. Psychol. Sci. 24 (1), 63–71. https://doi.org/10.1177/0956797612449175.
Wolbers, T., Hegarty, M., Büchel, C., Loomis, J.M., 2008. Spatial updating: how the brain keeps track of changing object locations during observer motion. Nat. Neurosci. 11 (10) https://doi.org/10.1038/nn.2189. Article 10.
Wu, X., He, S., Bushara, K., Zeng, F., Liu, Y., Zhang, D., 2012. Dissociable neural correlates of contour completion and contour representation in illusory contour perception. Hum. Brain Mapp. 33 (10), 2407–2414. https://doi.org/10.1002/hbm.21371.
Yamamoto, T., Takahashi, S., Hanakawa, T., Urayama, S., Aso, T., Fukuyama, H., Ejima, Y., 2008. Neural correlates of the stereokinetic effect revealed by functional magnetic resonance imaging. J. Vis. 8 (10) https://doi.org/10.1167/8.10.14, 14.1-17.
Zaretskaya, N., Anstis, S., Bartels, A., 2013. Parietal cortex mediates conscious perception of illusory gestalt. J. Neurosci. 33 (2), 523–531. https://doi.org/10.1523/JNEUROSCI.2905-12.2013.
Zeng, H., Fink, G.R., Weidner, R., 2020. Visual size processing in early visual cortex follows lateral occipital cortex involvement. J. Neurosci. 40 (22), 4410–4417. https://doi.org/10.1523/JNEUROSCI.2437-19.2020. The Official Journal of the Society for Neuroscience.